PERCOLATION IN CORRELATED SYSTEMS

BY VESSELIN MARINOV

A dissertation submitted to the

Graduate School—New Brunswick

Rutgers, The State University of New Jersey

in partial fulfillment of the requirements

for the degree of

Doctor of Philosophy

Graduate Program in Physics and Astronomy

Written under the direction of

Professor Joel L. Lebowitz

and approved by

_____

_____

_____

_____

New Brunswick, New Jersey

October, 2007

ABSTRACT OF THE DISSERTATION

Percolation in Correlated Systems

by Vesselin Marinov

Dissertation Director: Professor Joel L. Lebowitz

In this thesis we study various problems in dependent percolation theory. In the first part of this thesis we study disordered q-state Potts models as examples of systems in which there is percolation for an arbitrary low density and no percolation for arbitrary high density of occupied sites. In the second part of the thesis we study dependent percolation models in which the correlations between the site occupation variables are long range, i.e. decaying as r^{-a} for $a < d$, where r is the separation between any two sites and d is the dimension of the model. Scaling analysis suggests [1] that such long range correlated percolation models define a new percolation universality classes with critical exponents depending on a. We develop a field theoretic description of these models in an attempt to calculate the critical exponents of the transition in an double expansion in terms of $\epsilon = 6 - d$ and $\delta = 4 - a$. In the third part we study the percolation transition for two specific long range correlated percolation models on the 3 dimensional integer square lattice. These two percolation models are derived from the Voter model and the Harmonic crystal respectively. Our simulation results confirm the basic scaling arguments and the field theoretic results.

Acknowledgements

I would like to thank my PhD advisor Joel Lebowitz for introducing me to the wonderful world of percolation and for his guidance throughout the years of my PhD. He is a constant source of inspiration and new ideas. I would also like to thank Larry Zamick and Aram Mekjian for many interesting discussions we had about ‘ ‘elementary” physics problems while teaching the 323/324 course. Many thanks are also due to Lincoln Chayes for collaboration on the disordered Potts model; without him this part of the thesis would not have been in existence. I would also like to thank Greg Moore and Piers Coleman for sitting on my PhD defense committee and Eugene Speer for agreeing to be the external member on such a short notice. Thanks to my officemate Arvind Ayyer for enduring my negativity and always being ready for a discussion. Most of all I thank my wife Daniela for giving me the much needed moral support and love.

Dedication

To Teodor and Daniela

Table of Contents

List of Figures

Chapter 1

Introduction

In this thesis we confine our attention to the study of the percolation problems on the graph with sites $x \in \mathbb{Z}^d$ and edges connecting every two sites for which $|x - y| = 1$, where $|x| = |x_1| + |x_2| + \cdot + |x_d|$. In other words we take as the graph the usual d dimensional integer square lattice. Sites which are connected by an edge will be called nearest neighbor sites.

The first step in defining a percolation problem is to introduce a random percolation field η that lives on the sites or edges of this graph and takes values in $\{0, 1\}$. If the random field is defined on the sites of the graph then we speak of site percolation; if it is defined on the edges of the graph we refer to it as a bond percolation. A site $x \in \mathbb{Z}^d$ for which $\eta(x) = 1$ is called occupied and one for which $\eta(x) = 0$ it is called empty. In the case of bond percolation the terminology is open and closed, respectively. For clarity of exposition we will confine our discussion in this Introduction to site percolation.

The next step is to define a measure $\mathbf{P}$ on configurations $\eta \in \{0, 1\}^{\mathbb{Z}^d}$. A natural and easy to deal with measure is the product or Bernoulli measure. One refers to this as independent Bernoulli site percolation. One can however consider percolation problems in which the site occupation probability is assigned in some natural way which is not independent, i.e., in which the measure in question is not a product measure. This defines dependent or correlated percolation. In this thesis we will always consider $\mathbf{P}$ to be translation invariant.

Site percolation theory is concerned with the study of various statistics and properties of clusters of occupied sites that arise in a percolation model. A cluster in a given configuration is a maximal set of occupied sites such that one can reach any site from this set from any other site from this set by following a path consisting of nearest

neighbor bonds.

Although defined simply percolation provides many interesting problems. In particular it is an example of a second order phase transition. The phase transition in this case is marked by the existence, with probability one, of an infinite cluster of occupied sites if the density of occupied sites $p = \langle \eta(x) \rangle$ is in excess of some critical density p_c. The order parameter in this second order phase transition is the probability that a given site belongs to the infinite cluster. One is interested in calculating the critical exponents associated with this transition and identifying different universality classes.

There are many applications of percolation theory. It is used for the study of the spread of diseases, oil fields exploration, diffusion in disordered media, and random resistor networks. For a nice discussion of the applications of percolation theory see [2]. Percolation also has a very direct application in the study of the thermal phase transition of Ising type statistical mechanics spin models; we will discuss this in Chapter 2.

In this thesis we study various aspects of dependent percolation. In Chapter 2 we address the question whether there are some natural bounds for the critical percolation density p_c for percolation models on $\mathbb{Z}^2$. Using the disordered Potts model we provide examples of percolation models on $\mathbb{Z}^2$ for which p_c can be arbitrary close to 1 and models for which p_c can be arbitrary close to 0.

In Chapter 3 we turn our attention to long range correlated percolation models. These are models for which the occupation measure $\mathbf{P}$ has power law decaying two point correlations, i.e.,

$$\langle \eta(x)\eta(y) \rangle \sim |x-y|^{-a}. \tag{0.1}$$

Some time ago Weinrib and Halperin [3, 1] investigated this question for systems with such slow decay of the pair correlation. Their results, based on a generalization of the Harris criteria and confirmed by an ϵ-expansion, suggest that if the correlation between the occupation variables falls off as in (0.1) and if $a < d$, where d is the spatial dimension of the problem, then these correlations are relevant if $a\nu - 2 < 0$, where ν is the correlation length exponent for the associated independent percolation problem. Systems which satisfy the above criteria belong to a new universality class for which the percolation correlation length exponents is $\nu_{long} = \frac{2}{a}$. In Chapter 3 we develop

a different field theoretic description for the long range correlated percolation model from the one in [1] and perform a renormalization group calculation for its critical exponents. We confirm that up to two loops the prediction for the new correlation length critical exponent holds.

In Chapter 4 we study two models, the Harmonic Crystal and Voter model, which fall into the class of long range percolation models. We calculate through Monte Carlo simulation and finite size scaling the critical exponents associated with the percolation transition. For both these models $a = 1$ and our simulation results confirm that the correlation length critical exponent for both models is $\nu = 2$.

We conclude this thesis with some discussion of other topics of interest and further directions in Chapter 5

Chapter 2

The Percolation Threshold

2.1 Percolation Threshold for Independent Percolation

The simplest percolation models that we can define are the Bernoulli independent bond and site percolation models. In this section we deal with the Bernoulli independent bond percolation model on the d dimensional integer square lattice , and sketch the proof that for $d > 1$ there is a non-trivial percolation threshold p_c, i.e. $0 < p_c < 1$; we follow [4]. In section 2.3 we will discuss some dependent site percolation models derived from the q-state Potts Model for which one can have percolation for an arbitrarily small density and no percolation for an arbitrarily high density of occupied sites.

For independent Bernoulli bond percolation we declare independently each edge $e \in \mathbb{E}^d$ to be open with probability p and closed otherwise. Formally we consider the sample configuration space $\Omega = \prod_{e \in E^d} \{0, 1\}$. For an element $\omega \in \Omega$, $\omega(e) = 0$ corresponds to edge e being closed and $\omega(e) = 1$ corresponds of edge e being open. We take for the σ-algebra to be generated by the σ-algebra of finite dimensional cylinders of Ω. The probability measure on this space that we consider is $\mathbf{P}_p = \prod_{e \in E^d} \mu_e$ where $\mu_e(\omega(e) = 0) = 1 - p$ and $\mu_e(\omega(e) = 1) = p$.

A particular configuration of open edges defines a random subgraph of the d dimensional integer square lattice that contains the vertex set $\mathbb{Z}^d$ and all the open edges. The connected components of this subgraph are called open clusters. We will denote with $C(0)$ the open cluster that contains the vertex origin of $\mathbb{Z}^d$. Independent Bernoulli site percolation is defined similarly. In this case the sample space is $\Omega = \prod_{s \in Z^d} \{0, 1\}$. One can also consider a mixture of bond and site percolation: the percolation models that one can construct are only limited by ones imagination.

An important quantity of interest is the probability that $C(0)$ has an infinite number

of components. We will denote this probability by $P_\infty(p)$

$$P_\infty(p) = \mathbf{P}_p(|C(0)| = \infty) \tag{1.1}$$

$P_\infty(p)$ plays the role of the order parameter in the percolation "phase transition". To establish the existence of this transition one has to establish that $P_\infty(p) > 0$ for some values of the parameter p and $P_\infty(p) = 0$ for other values. In fact we are interested in finding a $0 < p_c < 1$ such that for $p > p_c$, $P_\infty(p) > 0$ and for $p < p_c$, $P_\infty(p) = 0$.

It is a trivial observation that if $d = 1$ then $P_\infty(p) = 0$ for any $p < 1$ and $P_\infty(p) = 1$ for $p = 1$. For $d > 1$ things are not so trivial and in this case $0 < p_c < 1$. For completeness of the exposition we will reproduce a proof of this statement [4].

We first prove that $p_c(d) > 0$. For a given configuration of open bonds, let $N(n)$ be the number of paths of length n that start from the origin and for which all bonds are open. Since the measure is a product measure $\langle N(n)\rangle = p^n\sigma(n)$ where $\sigma(n)$ is the number of paths in the d dimensional integer square lattice that start from a given point and have length n. We have the following inequality:

$$P_\infty(p) \leq \mathbf{P}_p(N(n) \geq 1) \leq \langle (N(n))\rangle = p^n\sigma(n) \tag{1.2}$$

It is trivial to prove that the connectivity constant of the d dimensional integer square lattice, $\lambda(d) = \lim_{n\to\infty} \sigma(n)^{\frac{1}{n}}$ is finite and satisfies the inequality $\lambda(d) \leq 2d - 1$. From the definition of the connectivity function we can conclude that $\sigma(n) = \{\lambda(d) + o(1)\}^n$ as $n \to \infty$. Substituting this in the last term of (1.2) we conclude that if $p\lambda(d) < 1$ then $P_\infty(p) = 0$. Thus we have proved that $p_c(d) \geq \frac{1}{\lambda(d)}$ and since $\lambda(d)$ is finite the result follows.

To prove that $p_c(d) < 1$ it is enought to prove that $p_c(2) < 1$ since $p_c(d) \geq p_c(d+1)$. To prove that $p_c(2) < 1$ we need to introduce the notion of the dual lattice. The dual lattice and dual models will be relevant for our discussions in section 2.3. For the case of the 2 dimensional integer square lattice the dual lattice is defined as follows. The nodes of the dual lattice reside at the center of the faces of the original lattice. We join all these nodes with edges if the corresponding faces share an edge of the original lattice. A part of the original 2 dimensional integer square lattice and its dual is drawn in Fig. 2.1. We declare an edge on the dual lattice to be open if the corresponding edge on the original

lattice that it crosses is closed and vice versa. This defines a bond percolation model on the dual lattice with edge probability $1-p$. It is not difficult to realize that if the cluster of occupied edges that belongs to the origin is finite, then necessarily there exist a closed circuit of open dual edges on the dual lattice that surrounds the origin, see Fig. 2.2 , and vice versa.

Let us denote with γ a circuit of bonds in the dual lattice that surrounds the origin and let us denote with $M(n)$ the number of such open circuits of size n. We have

$$\begin{aligned}\mathbf{P}_p(|C(0)|=\infty) &= \mathbf{P}_p(M(n)=0 \ \text{ for all } \ n) \qquad (1.3)\\ &= 1-\mathbf{P}_p(M(n)\geq 1 \ \text{ for some } \ n)\\ &\geq 1-\sum_{\gamma}\mathbf{P}_p(\gamma \ \text{ is open}).\end{aligned}$$

On the other hand

$$\begin{aligned}\sum_{\gamma}\mathbf{P}_p(\gamma \ \text{ is open}) &\leq \sum_{n=1}^{\infty}(1-p)^n n\sigma(n-1) \qquad (1.4)\\ &= \sum_{n=1}^{\infty}(1-p)n((1-p)\lambda(2)+o(1))^{n-1} \qquad (1.5)\\ &< \infty \ \text{ if } \ (1-p)\lambda(2)<1.\end{aligned}$$

The sum in (1.4) tends to zero if $p\to 1$ therefore there must exist an $\epsilon\in(0,1)$ such that

$$\sum_{\gamma}\mathbf{P}_p(\gamma \ \text{ is open}) \leq \frac{1}{2} \quad \text{if } \ p>\epsilon \qquad (1.6)$$

Combining (1.6) and (1.3) we find that $\mathbf{P}_p(|C(0)|=\infty)\geq\frac{1}{2}$ if $p\geq\epsilon$ and thus we conclude that $p_c(2)\leq\epsilon$. In fact using duality arguments one can conclude that for this 2 dimensional bond percolation model $p_c=\frac{1}{2}$ [4].

It is not so easy to prove the existence of a non-trivial percolation threshold when the occupation measure is not a product measure anymore. This problem is especially difficult when long range correlations are present. There has been some work on this subject, most notably [5] where the main result was the proof of the existence of a non-trivial percolation threshold p_c for the level field in the Harmonic Crystal in 3d. We will

discuss this problem further in Chapter 4, where we will use Monte Carlo simulations to numercialy identify p_c. Here we would like to note that one can easily extend the result in [5] for $d > 3$ [6]. To be concrete let us detail how this can be done. Let $\phi(x) \in \mathbb{R}$ be the massless Gaussian free field on $\mathbb{Z}^d$. The percolation field that we are interested in is defined as $\eta(x) = \mathbb{1}_{\phi(x)>h}$ with $h \in \mathbb{R}$. This field inherits the ergodicity of ϕ and it has finite energy [7]. If for a given level h there is a infinite cluster of occupied sites, we denote this cluster by C_∞, then this cluster is necessarily unique [7]. The density of this cluster $\rho(h)$ is then strictly positive [8]. The key element in the analysis in [5] is that if η percolates then $\langle \phi(x) \rangle > 0$. The same argument as in [5] can be used to prove this statement. In [5] the key observation is that in three dimensions any infinitely connected set is recurrent for a simple random walk. Having the extra information that for any dimension if there is an infinite cluster it has a positive density then again this cluster is recurrent for a simple random walk and the proof in [5] goes through.

Another model very similar to the Harmonic crystal is the Voter model. We will discuss this model further in Chapter 4. We have tried hard to find an argument that will support the existence of a non trivial percolation transition for this model but are unsuccessful so far. We however completed some Monte Carlo simulations from which one can conclude that this is the case; see Chapter 4.

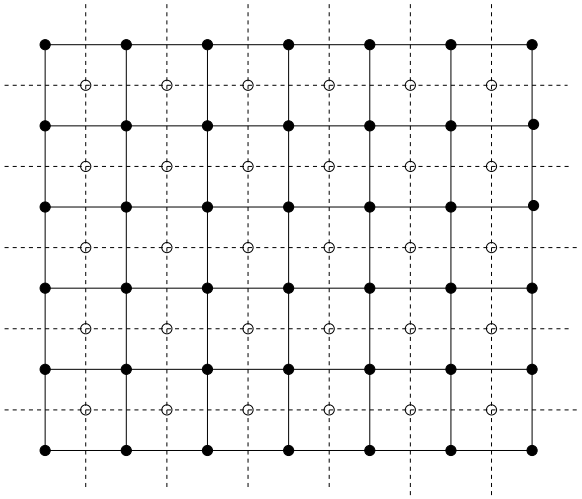

Figure 2.1: Part of the 2 dimensional integer square lattice together with its dual. The sites of the 2 dimensional integer square lattice are drawn as black dots while the sites of the dual lattice are drawn as empty circles

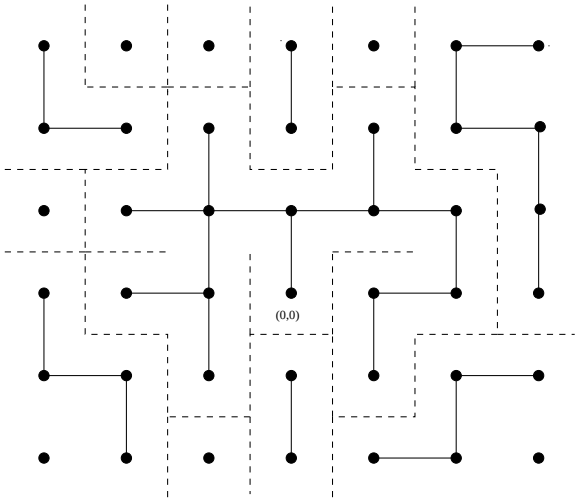

Figure 2.2: A random bond configuration of a percolation model on the 2 dimensional integer square lattice

2.2 The Potts Model and Percolation

The nearest neighbor Potts model is a natural generalization of the Ising model where the "spins" can take any number of q different values. In its most general form the model is defined by the Hamiltonian

$$H_{\mathbf{J}} = -\sum_{<i,j>} J_{i,j}\delta_{\sigma_i\sigma_j} \tag{2.1}$$

where $\langle i,j\rangle$ denotes nearest neighbors, $J_{i,j}$ are real numbers which represent the strength of interaction between sites i and j, and $\sigma_i \in \{1...q\}$ is the value of the "spin" at site i. We will denote by $\mathbf{J}$ the collection of couplings $\{J_{i,j}\}$. The model could in general be defined on an arbitrary graph but for our discussion we will concentrate on d dimensional integer square lattice. Later on we will allow $J_{i,j}$ to be a collection of iid non-negative random variables with a common distribution F; in this case we will refer to the model as the disordered Potts Ferromagnet.

The Gibbs measure for this model in a finite volume with specified boundary conditions is defined as usual. Namely, if $\Lambda \subset \mathbb{Z}^d$ and the boundary $\partial\Lambda$ has fixed boundary spins $\sigma_{\partial\Lambda}$ we write

$$\mathbb{P}^{\sigma_{\partial\Lambda}}_{\mathbf{J},\Lambda}(\sigma_\Lambda) \propto e^{-H_{\mathbf{J}}(\sigma_\Lambda|\sigma_{\partial\Lambda})} \tag{2.2}$$

where $H_{\mathbf{J}}(\sigma_\Lambda|\sigma_{\partial\Lambda})$ is the expression (2.1) restricted to the sites in $\Lambda \bigcup \partial\Lambda$ with $\sigma_{\partial\Lambda}$. One can consider various boundary conditions; the most useful ones are when we consider all $\sigma_i \in \partial\Lambda$ be fixed to one of the q spin values (since the Hamiltonian is symmetric it does not matter which one we choose). The second choice of interest is the so called free boundary conditions: defined by taking $J_{i,j} = 0$ whenever $i \in \Lambda$ and $j \in \partial\Lambda$. Note that we have absorbed the inverse temperature β in the definition of $J_{i,j}$.

The phase transition in such systems is signaled by the non-uniqueness of the infinite volume limit of the Gibbs measure (2.2), see [9]. In this section we are going to describe the so called Random Cluster Measures which are an important tool for the rigorous study of these models.

The random cluster model, also known as the Fortuin-Kasteleyn (FK) model, is a dependent percolation model depending on two parameters $\mathbf{R}$ and q, $\mathbf{R}$ is a vector of

parameters $R_{i,j}$, one for each edge $\langle i,j\rangle$ in the collections of edges $\mathcal{E}$ in a finite graph $\mathcal{G}$ and q is some positive real number. For each configuration ω of open and closed bonds on $\mathcal{E}$ the FK measure assigns the following probability

$$\mathbf{P}_{\mathbf{R},q} \propto \{\prod_{e\in\mathcal{E}} R_e^{\omega(e)}(1-R_e)^{1-\omega(e)}\}q^{c(\omega)} \tag{2.3}$$

where $R_e \in [0,1]$ for all $e \in \mathcal{E}$ and $q > 0$, and $c(\omega)$ is the number of clusters (connected components) in the subgraph defined by the bonds for which $\omega(e) = 1$. In principle one needs to discuss the issue of boundary conditions which have impact on the calculation of $c(\omega)$, but this leads to unecessary complications for the purpose of the current discussion. We will revisit these random cluster measures in Sec. 2.3.3 , where we discuss boundary condition in more detail. Note that for $q = 1$ the above measure reduces to the Bernoulli bond percolation measure. This observation together with the relation between the FK measures and Potts models that we will establish below is the base of the claim that percolation is the $q \to 1$ limit of a q-state Potts model. This observation can be used to build a field theoretic description of the percolation "phase transition"; we discuss this in Section 3.3.

For non zero q the FK measure exhibits correlations. If we take $q \in \{2,3,...\}$ one obtains a random cluster measure that is ultimately related to the measure of the corresponding q-state Potts model. The relation between these two measures is realized by the so called Edwards-Sokal measure [9]. Edwards-Sokal measure is a coupling between the random cluster model with parameters q and $\mathbf{R}$, and the q-state Potts model with collection of couplings $\mathbf{J}$ such that $\mathbf{R} = 1 - e^{-\mathbf{J}}$. A coupling is a measure defined on the joined probability space for the two measures such that its two marginals are exactly the two given measures. To each element $(\sigma,\omega) \in \{1,...,q\}^{\mathcal{V}} \times \{0,1\}^{\mathcal{E}}$, here $\mathcal{V}$ is the vertex set of $\mathcal{G}$, the Edwards-Sokal measure assign the probability

$$\prod_{e=<x,y>\in\mathcal{E}} R_e^{\omega(e)}(1-R_e)^{1-\omega(e)} I_{(\sigma(x)-\sigma(y))\omega(e)=0}\,. \tag{2.4}$$

That is the measure assigns non-zero probability only to configurations for which if two sites are connected with an open bond then they necessarily have the same spin.

One useful application of this coupling is the construction of an effective simulation

algorithm for q-state Potts models [9]. The basis of this algorithm lies in the following Theorem that we adopt from [9]:

Theorem 2.2.1 *Let $R_{i,j} = 1 - e^{-J_{i,j}}$, and suppose we pick a random spin configuration $\sigma \in \{1, ..., q\}^{\mathcal{V}}$ as follows*

1. Pick a random edge configuration $\omega \in \{0,1\}^{\mathcal{E}}$ according to the random-cluster measure $\mathbf{P}_{\mathbf{R},q}$.

2. For each connected component C of ω, pick a spin at random (uniformly) from $\{1, ...q\}$, assign this spin to every vertex of C, and do this independently for different components.

Then σ is distributed according to the Potts model Gibbs measure $\mathbb{P}_{\mathbf{J}}$.

We note here that the random cluster representation only works for the case of zero external field, since then all the different "spins" are equivalent.

Theorem 2.2.1 provides us with a route to proving the existence and deriving various properties of the limit of finite volume Gibbs measures of the q-state Potts model. One first proves the existence of such limit for the random cluster measure, associate with the q-state Potts model and then using 2.2.1 one obtains the limit for the Gibbs measure. The random cluster measures enjoy certain monotonicity properties which makes them easy to deal with, see [9] and the Appendix in [10]

As is well know, non-uniqueness in the infinite volume Gibbs measure signals the existence of a phase transition. Another nice application of the random cluster measures is a characterization of thermal phase transition in a Potts spin model in terms of percolation in the associated random-cluster model [9], see also Sec. 2.3.3.

2.3 Percolation in High and Low Density Systems

In this section we address the question of whether there are "natural" translation and (lattice) rotation invariant ergodic measures on configurations $\eta \in \{0,1\}^{\mathbb{Z}^d}$, $d \geq 2$, for which site percolation occurs when the density of occupied sites, $p = \langle \eta_i \rangle$, is very close to zero and/or fails to occur if the density is close to one. It is known that neither phenomenon occurs for systems with product measures (independent percolation) [9, 4],

where, in most situations, there is a sharp percolation transition when p^{-1} is of the order of the lattice coordination number (e.g. $2d$). The question then is what happens when the occupancy of different sites is specified in some natural way which is *not* independent. Of particular interest are equilibrium spin–systems and non-equilibrium stationary states of interacting particle systems such as the voter model, the contact process and their various generalizations [11]. Furthermore, one may also consider projections of such measures, i.e. given a measure on $[\Omega]^{\mathbb{Z}^d}$, where $\sigma_i \in \Omega$ is the set of possible states at $i \in \mathbb{Z}^d$, we define an occupation variable $\eta_i = 0, 1$, with $\eta_i = 1$ if $\sigma_i \in \Omega_1$ and $\eta_i = 0$ if $\sigma_i \in \Omega \setminus \Omega_1$. Well known examples are the fuzzy q-state Potts model with $q = r + s$ and $\eta_i = 1$ if $\sigma_i \in (1, .., r)$, and systems where $\sigma_i \in \mathbb{R}$, and $\eta_i = 1$ if $\sigma_i \geq h$ and zero otherwise [12, 13, 5].

Adams and Lyons [14] considered these types of question for measures on homogeneous trees that are invariant under the graph automorphisms. They found that whenever the density is large enough there indeed is percolation, see also [15] and [16]. Such a result does *not* hold for $\mathbb{Z}^d$; it is easy to construct counter examples which exploit, in an obvious way, the vanishing surface to volume ratio of regular sets [9]. Also, for $d = 2$ one may consider an independent percolating cluster near threshold and simply declare the complimentary sites to have $\eta_1 \equiv 1$; these complimentary sites will have density close to one and fail to percolate. Higher dimensional analogs may even be possible, albeit at different thresholds (c.f. [17]) and the converse phenomenon can also be constructed by these means: Consider a slightly super–critical percolating cluster and declare its compliment to be vacant ($\eta_i \equiv 0$). While such examples are not particularly interesting in their own right, they demonstrate the existence of mechanisms for these phenomena which might occur in more realistic systems.

In this section, the principal system under study is the $2d$ disordered Potts ferromagnet. First we will demonstrate that at self–dual critical points there is an absence of percolation despite a density which may be arbitrarily close to one. The complimentary result, namely percolation at small density, would follow immediately from continuity of the magnetization – a currently open and challenging problem. (We will state some *inconclusive* results concerning this question.) However, almost trivially, the

diluted versions of the disordered Potts models exhibit this property throughout the low temperature phase provided the system itself is near threshold; we will provide a formal proof. Finally we will combine the two sets of results via the consideration of models with *strong* and *weak* interactions. These models inherit enough of the features of the dilute model to display the small density percolation property yet, unlike the dilute models, can have a self–dual point.

Most of the above stated results are proved in the context of a fixed realization of the disorder. However, since any particular realization is not translation invariant we do not satisfy the naturalness criterion that was stated at the beginning of this section. Therefore we will consider the entire problem from the perspective of the *quenched* measures. These objects are manifestly translation invariant and we will demonstrate various other properties, such as strong mixing.

The remainder of this section is organized as follows: We first define the general quenched disordered Potts ferromagnets but with the emphasis on $d = 2$. We define the *quenched measures* for these systems; certain general properties of these quenched measures are stated; the proof of these can be found in the Appendix of [10]. We then prove our main results: (i) At certain self–dual critical points, any one of the species is sufficient to prevent percolation of the combined efforts of all the others. (ii) For the dilute model, with the active bonds in slight excess of the percolation threshold, there is a non–trivial low temperature phase characterized by the percolation of just one of the species notwithstanding (for $q \gg 1$) the paucity of the overall density of this species. Finally we construct a weak–bond/strong–bond disordered model with a self–dual point *and*, at least in the vicinity of the transition temperature, a regime of percolation at low density. In the next section, we will provide some discussion. For further background discussion, see [9] Section 5.2.

2.3.1 Disordered Potts Ferromagnets

The Disordered Potts Ferromagnet is defined as in (2.1) but now the couplings $J_{i,j}$ are considered to be iid non-negative random variables with common distribution F not concentrated at a single point; we emphasize that we may allow $J_{i,j} = 0$ with non-zero

probability, a case we will refer to as dilution.

For finite volume, the quenched measures are defined by averaging the probabilities in (2.2) over all realizations of the interactions according to $\prod_{\langle i,j\rangle} dF(J_{i,j})$ (written as dF) – where the product runs over the appropriate set, usually i and j in $\Lambda \cup \partial\Lambda$). These averaged objects will be referred to as the finite volume *quenched* measures and denoted by $\mathbb{Q}^{\sharp}_{F;\Lambda}$ with the superscript denoting one of the two types of boundary conditions described, i.e., $\sharp = [1]$ corresponds to fixing the value of the spins at the boundary to 1 and $\sharp = [f]$ corresponds to free boundary conditions. As far as infinite volume limits are concerned, there are two alternative scenarios: (1) for fixed $\mathbf{J}$ take $\Lambda \nearrow \mathbb{Z}^2$ and (somehow) average the resultant measure over $\mathbf{J}$. (2) Take the (vague) infinite volume limit of the finite volume quenched measures described above. It turns out that for the pertinent cases at hand, the order of the procedures is immaterial and the result is independent of how $\Lambda \nearrow \mathbb{Z}^2$. We will provide a brief sketch of how this is established in the appendix.

Below we summarize our claims concerning these quenched measures; the proofs for these can be found in [10].

Proposition A1 *For all F satisfying the ferromagnetic condition, that is $J_{i,j} \geq 0$ with probability one, the limiting measures*

$$\mathbb{Q}^{[1]}_F = \lim_{\Lambda \nearrow \mathbb{Z}^2} \mathbb{Q}^{[1]}_{F;\Lambda} \tag{3.1}$$

exists (independently of how $\Lambda \nearrow \mathbb{Z}^2$) and similarly for $\mathbb{Q}^{[f]}_F$. Furthermore, the measures $\mathbb{Q}^{[1]}_F$ and $\mathbb{Q}^{[f]}_F$ are invariant under $\mathbb{Z}^2$ shifts – as well as other $\mathbb{Z}^2$ symmetries.

Proposition A2 *If $\mu^{[1]}_{\mathbf{J}}$ and $\mu^{[\mathrm{f}]}_{\mathbf{J}}$ are limiting Gibbs measures (which also exist independently of how the infinite volume limit is taken) then the average of these measures is well defined and equal to their respective $\mathbb{Q}$ counterpart. Finally, if F is such that the spontaneous magnetization as defined thermodynamically (or as will be discussed subsequent to Eq.(3.7)) is zero then the limiting quenched measure – satisfying all properties of Proposition A1 above and A3 below – is unique.*

Proposition A3 *The limiting measure $\mathbb{Q}^{[1]}_F$ satisfies the strong mixing condition. So, in particular, if the magnetization vanishes the unique measure is strongly mixing.*

While most likely these are non–Gibbsian measures, as is evidenced by the result in [18] on a related system, they are physically motivated and, possibly, experimentally accessible. Notwithstanding, at self–dual points (and presumably at other critical points) the combined efforts of species 2 through q will fail to achieve percolation in spite of their high density. Furthermore in the dilute case (and related cases) despite a low density, the type–1 spins can, on their own, achieve percolation in the $Q_F^{[1]}$ – measures.

2.3.2 Statement of Main Results

For $0 < J < \infty$, the dual coupling is defined by

$$J^*(J) = \log\left(1 + \frac{q}{e^J - 1}\right). \tag{3.2}$$

and the dual model is defined by the assignment of the coupling $J^*(J_{i,j}) \equiv J^*_{i,j}$ to the bond $\langle i^*, j^*\rangle$ of the dual lattice $(\mathbb{Z} + \frac{1}{2})^2$ that is traversal to the bond $\langle i, j\rangle$. A model is self–dual [1] if

$$dF(J_{i,j}) = dF(J^*_{i,j}). \tag{3.3}$$

Our result on the bond–random Potts ferromagnets reads as follows:

Theorem 2.3.1 *Suppose that for the ferromagnetic bond strength distribution F, in both the direct and the dual model, the spontaneous magnetization vanishes. Then, with probability one, in the (unique) limiting quenched measure there are infinitely many circuits surrounding the origin such that the spin–type is constant throughout the circuit and, moreover, there are infinitely many such circuits of each spin–type. In particular, there is no percolation (or even $*$–percolation) in the various marginal measures which identify as many as $(q-1)$ of the spin–states as a single state notwithstanding that the density of this amalgamation is $1 - \frac{1}{q}$*

Corollary 2.3.2 *For a 2D disordered Potts model at a point of self–duality, the (hypotheses and) conclusions of Theorem 2.3.1 hold.*

---

[1] For models that do not respect all of the $\mathbb{Z}^2$ symmetries, a more general definition of self–duality is possible e.g. the vertical bonds distributed as the dual of the horizontal bonds and vice versa. While most of our results go through easily in these cases, we make no further reference to these extensions since the present purpose is to construct "natural measures" on $\mathbb{Z}^2$

Our next result concerns situations which *do* have percolation:

Theorem 2.3.3 *Consider the dilute model with parameters a and β defined by $J_{i,j} = \beta$ with probability a and zero otherwise. If $a > \frac{1}{2}$ there is a $\beta_c < \infty$ such that for all $\beta > \beta_c$, the magnetization $m(\beta, a)$, given for [1] boundary conditions by the excess density of species 1 above $\frac{1}{q}$, satisfies the inequalities*

$$0 < m(\beta, a) < P_\infty(a) \tag{3.4}$$

where $P_\infty(a)$ is the percolation probability in the independent bond–model on $\mathbb{Z}^2$. In particular, for all $\beta > \beta_c$, in the measure $Q_F^{[1]}$, there is (with probability one) an infinite cluster of species 1 while the overall density of this species is $m(\beta, a) + \frac{1}{q} \leq P_\infty(a) + \frac{1}{q}$; by considering large q and a close to $\frac{1}{2}$, this density can be made as small as desired.

Both features may be exhibited in a single model:

Theorem 2.3.4 *Consider a disordered Potts ferromagnet with strong and weak bonds, e.g. $J \geq b$ with probability a and $J = J^*(J)$ with probability $(1 - a)$. Then for b large, the magnetization is very nearly $P_\infty(a)$ and the overall density in the measure $Q_F^{[1]}$ is very nearly $P_\infty(a) + \frac{1}{q}$. Since the model is self–dual at $a = \frac{1}{2}$, both the high and low density percolative phenomena occur as the parameter a passes through $\frac{1}{2}$.*

2.3.3 Graphical Representations, Dual Models and Dominations

For $\langle i, j \rangle$ a neighboring pair let us define

$$R_{i,j} = e^{J_{i,j}} - 1. \tag{3.5}$$

As is well known [19], see also Sec. 2.2 the model admits the *random cluster* representation: In finite volume, if ω is a configuration of occupied and vacant bonds (or edges) the probability of ω is given by

$$\mathbf{P}^\sharp_{\mathbf{J};\Lambda}(\omega) \propto \prod_{\langle i,j \rangle \in \omega} R_{i,j} q^{c^\sharp(\omega)} \tag{3.6}$$

where $\langle i, j \rangle \in \omega$ represents the event that the particular bond is occupied and $c^\sharp(\omega)$ denotes the number of connected components which are counted by rules ($\sharp$) in accord

with conditions specified at the boundary: $\sharp = [1]$ and $\sharp = [\mathrm{f}]$. In the former case – sometimes called the *wired* measures – $c^{[1]}(\omega)$ counts all clusters that are attached to the boundary as part of the same connected component while $c^{[\mathrm{f}]}(\omega)$ simply counts the number of components in ω by the conventional definition. Given these random cluster measures it is possible to write down the conditional probabilities of spin configurations given a bond configuration. This is done by insisting that the spin–value is constant throughout each component of ω and, except for the components attached to the boundary, assigning the spin–types to each component independently and with equal probability. As for the boundary component, as far as concern the two setups in this work the procedures are simple: For [f], nothing special is done – all boundary components are treated like the internal components. For the wired or [1] case, all components of the boundary are set to the first spin–state. Thus, for example, the finite volume magnetization at the origin for specified $\mathbf{J}$ is given by

$$m_{\mathbf{J};\Lambda}(0) \equiv \mathbb{E}^{[1]}_{\mathbf{J};\Lambda}(\delta_{\sigma_0,1}) - \frac{1}{q} = \mathbf{P}^{[1]}_{\mathbf{J};\Lambda}(\{0 \leftrightarrow \partial\Lambda\}) \tag{3.7}$$

where $\{0 \leftrightarrow \partial\Lambda\}$ is the event that the origin is connected to $\partial\Lambda$ by an occupied path. The average magnetization at the origin $\bar{m}^{[1]}_{\Lambda}(0)$ is obtained by averaging (3.7) over F. The infinite volume spontaneous magnetization $\bar{m}^{[1]}(0)$ is obtained by taking the limit $\Lambda \nearrow \mathbb{Z}^d$ of $\bar{m}^{[1]}_{\Lambda}(0)$. We call $\bar{m}^{[1]}(0)$ the spontaneous magnetization of the system.

To conclude: on the basis of Eq.(3.7) the magnetization at the origin is non–zero in any given quench (realization) if and only if the right hand side does not tend to zero as $\Lambda \nearrow \mathbb{Z}^2$; i.e. percolation and spontaneous magnetization are synonymous. That the limiting percolation density exists (with or without the quenched average) is well known and anyway can be derived on the basis of what is discussed later. The fact that percolation probability is equal to the thermodynamically defined spontaneous magnetization has been proved elsewhere, see [20] and references therein, as well as [21] and [22].

In finite volume, the dual model is defined as follows: If $\langle i, j\rangle$ is an edge of $\mathbb{Z}^2$, let $\langle i^*, j^*\rangle$ denote the corresponding edge of $(\mathbb{Z} + \frac{1}{2})^2$ and let

$$R^*_{i^*,j^*} = \frac{q}{R_{i,j}}. \tag{3.8}$$

which is the equivalent of Eq.(3.2). For a finite $\Lambda \subset \mathbb{Z}^2$ – with Λ regarded as a graph – consider the dual graph, Λ^* consisting of all (dual) edges corresponding to those (direct) edges in Λ and the collection of (dual) sites which are the endpoints of these dual edges. As is well known, the model on the dual graph with parameters $R^*_{i^*,j^*}$ has configurations which are in one–to–one correspondence with (and have the same probabilities as) the original setup on Λ. Of course, some attention must be paid to the conditions at the boundary. All that is needed in this work is the readily verified fact that the model with wired boundary conditions on Λ associates with the model with free boundary conditions on Λ^* and vice versa. We will refer to the initial model as the *direct* model and the induced distribution for the $J^*_{i^*,j^*}$ – collectively denoted by $\mathbf{J}^*$ – by $\mathbb{F}^*$. Of course when it comes to integration, we may use the "direct" dF.

A model is said to be *self–dual* if the probability distribution of the $\{J^*_{i,j}\}$ is the same as that of original e.g. the Eq.(3.3) or, equivalently,

$$R_{i,j} =_d \frac{q}{R_{i,j}} \tag{3.9}$$

The "nicest" examples concern a self–duality which is achieved according to a temperature parameter, in which case one can speak of the self-dual temperature $\bar{\beta}$, c.f. Eq.(30) in [23], but this will not be necessary in the present work.

For the sake of completeness, let us recapitulate in brief (special cases of) the domination arguments that were derived in [21, 22]. For fixed bond $\langle i, j\rangle$ in finite volume with free or wired boundary conditions, let us calculate the conditional probability that the bond is occupied. It is not hard to see that this is exactly

$$p_{i,j} = \frac{R_{i,j}}{1 + R_{i,j}} \tag{3.10}$$

if $\{i \leftrightarrow j\}$ while the probability is

$$p^{\text{eff}}_{i,j} = \frac{R_{i,j}}{q + R_{i,j}} = \frac{p_{i,j}}{p_{i,j} + q(1 - p_{i,j})} \tag{3.11}$$

if the endpoints are not connected. (In the former, the number of components is unaffected while in the latter, it is reduced by one.) It therefore follows from elementary considerations that for each quench, the random cluster measures – wired or free –

dominate the independent bond measures at parameters $p_{i,j}^{\text{eff}}$ and are dominated by independent bond measures with parameters $p_{i,j}$. The ease of calculating quenched averages of independent bond measures (percolation on percolation) is what lead to the asymptotically sharp results of [22]. Indeed, as is already seen, when the relevant R–parameter is large compared with q, the upper and lower estimates do not differ by much.

2.3.4 Proofs of Main Results

We start with a preliminary result which is most of what is needed for the proof of Theorem 2.3.1

Proposition 2.3.5 *Let F denote a distribution of couplings such that the spontaneous magnetization of the dual model is zero. Then with probability one for both $\mathbb{Q}_F^{[1]}$ and $\mathbb{Q}_F^{[f]}$ there are infinitely many circuits surrounding the origin such that, within each circuit, the spin–type is constant.*

Proof. Let $\epsilon > 0$ and let $\tilde{V} \subset \mathbb{Z}^2$ denote a finite set containing the origin. Let $\tilde{\Lambda} \supset \tilde{V}$ and $\mathcal{D}_{\tilde{V},\tilde{\Lambda}}$ denote the event

$$\mathcal{D}_{\tilde{V},\tilde{\Lambda}} = \{\sigma \mid \exists \text{ a circuit of constant spin–type separating } \partial\tilde{V} \text{ and } \partial\tilde{\Lambda}\}. \tag{3.12}$$

Then it is sufficient to prove (for arbitrary fixed $\tilde{V}$ and ϵ) that $\mathbb{Q}_F^{[\mathrm{f}]}(\mathcal{D}_{\tilde{V},\tilde{\Lambda}}) > 1 - \epsilon$ whenever $\tilde{\Lambda}$ is sufficiently large, and similarly for $\mathbb{Q}_F^{[1]}$. We let V – and Λ – denote sets similar to their tilde counterparts enhanced by a layer or two at the boundary to avoid discussion of inconsequential provisos caused by discrete lattice effects. Let Λ^* and V^* denote the dual sets and let $\Upsilon = \frac{\epsilon}{|\partial V^*|}$. Since the quenched magnetization in the dual measure vanishes by hypothesis, then for every $i^* \in \partial V^*$ the average magnetization at i^* in the one–boundary conditions in Λ^* (for the dual model) tends to zero as Λ^* gets large. Thus, in a large enough volume,

$$\overline{m}_{F^*;\Lambda^*}(i^*) \equiv \int dF\, \mathbb{E}^{[1]}_{\mathbf{J}^*;\Lambda^*}(\sigma_{i^*} - \frac{1}{q}) < \Upsilon \tag{3.13}$$

However, according to Eq.(3.7), the integrand is the probability, in the dual model, of

a dual connection between i^* and $\partial\Lambda^*$. Thus

$$\int dF\, \mathbf{P}^{[1]}_{\mathbf{J}^*;\Lambda^*}(\{\partial V^* \leftrightarrow \partial\Lambda^*\}) \leq \int dF \left[\sum_{i^* \in \partial V^*} \mathbf{P}^{[1]}_{\mathbf{J}^*;\Lambda^*}(\{i^* \leftrightarrow \partial\Lambda^*\}) \right] \leq |\partial V^*| \Upsilon \leq \epsilon. \tag{3.14}$$

However, $1 - \mathbf{P}^{[1]}_{\mathbf{J}^*;\Lambda^*}(\{\partial V^* \leftrightarrow \partial\Lambda^*\})$ is the probability in the direct model of an occupied circuit separating ∂V from $\partial\Lambda$ in the transformed boundary conditions. So we may write

$$\int dF\, \mathbf{P}^{[f]}_{\mathbf{J};\Lambda}(\{\exists \text{ occupied circuit separating } \partial V \text{ and } \partial\Lambda\}) \geq 1 - \epsilon. \tag{3.15}$$

But each spin realization associated with such a random cluster event has a circuit of the desired type and we have obtained the desired result in finite volume with free boundary conditions:

$$\mathbb{Q}^{[\mathrm{f}]}_{F;\Lambda}(\mathcal{D}_{\tilde{V},\tilde{\Lambda}}) \geq 1 - \epsilon. \tag{3.16}$$

The result for infinite volume follows by monotonicity of the integrand in Eq. (3.15) in the system size: As discussed in the appendix, for free boundary conditions, the integrand increases when we consider the same event (involving $\partial\Lambda$) in a volume $\Lambda' \supset \Lambda$. For wired boundary conditions, the result follows because the in any volume, the integrand increases if we replace [f] by [1]. □

Proof of Theorem 2.3.1 Since the dual magnetization vanishes we already have, according to the previous proposition the part concerning the infinitely many circuits. What is lacking is a proof that these circuits are not not all of the same spin–type (as would indeed be the case if the spontaneous magnetization were positive). Now, using the fact that the direct magnetization also vanishes, we may demonstrate, along the lines of Equations (3.14) through (3.16) that outside any finite V but inside a sufficiently large Λ the average probability of observing the dual of a circuit composed of *vacant* bonds is close to one – even with (direct) wired boundary conditions.

The upshot, when both magnetizations vanish, is that even in finite volume, with high probability many circuits of dual bonds and many circuits of direct bonds surround the given V. Since both the direct and dual circuits can be "freshly constructed" at an increasing sequence of scales, it follows that some portion of these circuits separate each other. There are many direct rings separated from each other (and the boundary)

by the dual rings. These direct rings are therefore "at liberty" to take on any of the q spin–values. In particular for any $s \in \{1, \dots q\}$ and any finite V,

$$\mathbb{Q}^{[1]}_{F;\Lambda}(\{\exists \text{ a circuit of spin–type } s \text{ surrounding } V\}) \longrightarrow 1 \tag{3.17}$$

as $\Lambda \nearrow \mathbb{Z}^2$. The result also holds in $\mathbb{Q}^{[\mathrm{f}]}_{F;\Lambda}$ (which anyway leads to the same limiting measure as we show in Proposition A2). The conclusion is that with probability one, in the limiting measure there are infinitely many circuits of all types surrounding the origin. This establishes the first claim. It also establishes the absence of percolation for any amalgamation–alliance since an infinite path (connected or $*$–connected) of the alliance without the s^{th}spin–state, starting from the origin, is prevented by any of the s^{th} state's circuits, the presence of which has probability one. Finally, as is evident from the absence of magnetization, the population density of all species is exactly $\frac{1}{q}$. □

Proof of Corollary 2.3.2 As was demonstrated in [23], Theorem 1′, the magnetization of the disordered 2D Potts models vanishes at self dual points. This applies equally well to the dual model. □

Proof of Theorem 2.3.3 This result is, to the largest extent, contained in [22] so we will be succinct. In a given quench, each edge corresponding to a zero coupling bond adds nothing to the ferromagnetism. The active bonds must be "reoccupied" with a conditional probability bounded above by $R/[1+R]$ and below by $R/[q+R]$ where $R = e^{\beta} - 1$. The fraction of these reoccupied bonds that belong to an infinite cluster (in the limiting [1]–state) constitute the magnetized fraction. After performing a quenched average, it is seen that the magnetization is positive whenever

$$a\frac{R}{q+R} > \frac{1}{2} \tag{3.18}$$

but is bounded above by $P_\infty(\frac{aR}{q+R}) < P_\infty(a)$. This is small and positive for all β large enough and a close to $\frac{1}{2}$. The density of ones, in the one state is just this magnetization plus the ambient $\frac{1}{q}$. □

Proof of Theorem 2.3.4 For simplicity we will treat just the case where with probability a, $R = e^J - 1 = e^b - 1 \equiv B$ and with probability $(1-a)$, $R = q/B$. Obviously, for

$a = \frac{1}{2}$, the model is self–dual. To prove the remaining statements, we reiterate that

$$P_\infty(p^{\text{eff}}) \leq m(B, a) \leq P_\infty(p) \tag{3.19}$$

where, in general, $p^{\text{eff}} = \int dF[R/(q+R)]$, etc. Thus it is sufficient to find B and a such that both p^{eff} and p are in slight excess of $\frac{1}{2}$. In this simple case, we may write

$$p^{\text{eff}} = a\frac{B}{B+q} + (1-a)\frac{1}{1+B} \tag{3.20}$$

and

$$p = a\frac{B}{1+B} + (1-a)\frac{q}{B+q}. \tag{3.21}$$

It is readily seen that that when $a \gtrsim \frac{1}{2}$ and $B \gg q$ the desired conditions are met. □

2.3.5 Conclusion

We have shown that for the disordered ferromagnetic q-state Potts model on $\mathbb{Z}^2$ at points of self–duality there is no percolation for any amalgamation of $q-1$ components in the unique translation invariant mixing measure $\mathbb{Q}_F$. This transpires despite the fact that the density of these combined $q-1$ states is $1-q^{-1}$ which will be arbitrary close to 1 as $q \to \infty$. Of course we expect that the above holds at all critical points of these models. In particular, we suppose, on general grounds, that the conditions of Theorem 2.3.1 (namely no percolation and no dual percolation in the graphical representation) holds at any critical point in a model of this sort.

It is further expected that as soon as the temperature is decreased below the critical temperature or the overall interaction strength increased, the magnetization will rise continuously from zero. If this scenario is correct, i.e. if the magnetization (like the energy density) is continuous for this system, it would follow that in each of these states we would have percolation at a small density.

Unfortunately, even aided with self–duality, we cannot make such an assertion. We may use duality for the weaker assertion that the magnetization is not already positive at a self–dual point (c.f. the discussion in [24]). Indeed, this would imply the identical circumstance in the dual model – with appropriately modified boundary conditions – and the latter would be a non–percolative state from the perspective of the direct

model which would mean the existence of two states with differing energy density which is ruled out by the result of [25]. More succinctly, there cannot be a point where the model exhibits a percolative and a non—percolative state – so the magnetization indeed vanishes at a self–dual point. But this does not quite rule out the possibility of a critical interval surrounding a self–dual point with a magnetic discontinuity at the endpoint and *no* associated non–percolative state.

Trivial examples of discontinuous order parameters coinciding with critical transitions are abundant in short–range 1D systems at zero temperature e.g. the Ising model. The energy is continuous as $T \downarrow 0$ but $m(0) = 1$. More intricate examples can be found, here we mention two. First there is the (reinterpretation of the) mean–field k–core transition [26] where, in the presence of two distinct divergent length scales – and susceptibilities – there is a discontinuity in the order parameter. Second, we mention the well known Thouless effect [27] for the 1D Ising model with ferromagnetic pair–interactions that decay like the inverse square of the separation. Here, as was proved in [21], the magnetization is discontinuous at the transition point but this point is critical in the sense of a divergent length scale, a divergent susceptibility and, it is presumed, a continuous energy density. It is interesting to note that, from the low temperature side, this transition is indeed the endpoint of a critical phase [28, 29].

In our study we have circumvented these mathematical intricacies and demonstrated percolation at small densities by considering dilute and "nearly dilute" models. In the former case, the magnetization is always small and in the latter case, it is demonstratively small in the vicinity of the critical point. This certainly does not settle the issue of magnetic/percolative continuity in these models, but it does, perhaps, bring us a small step closer.

Chapter 3

Critical Exponents, Long Range Correlated Percolation and the Renormalization Group

3.1 Critical Exponents

Once a percolation transition is identified as discussed in Chapter 2 one can think of various questions concerning the structure of the clusters above and below the percolation threshold. Various quantities of interest diverge as one approaches the critical density p_c. In the rest of this thesis we study a small subset of such quantities and the associated critical exponents.

The first quantity of interest is the percolation probability $P_\infty(p)$ which was defined in Chapter 2. For the case of independent percolation it can be shown that $P_\infty(p)$ is a continuous function [4]. This is the order parameter of the percolation transition; it vanishes for $p < p_c$ and is non zero for $p > p_c$

A second quantity of interest is the average cluster size $\kappa(p) = \langle |C(0)| \rangle$, where the average is over the occupation probability $\mathbf{P}$; this is analogous to the succeptability in spin models. For $p > p_c$ we have $P_\infty(p) > 0$ and thus $\kappa(p)$ diverges for these values of the site occupation density. For independent percolation it can be rigorously proved that the point at which $\kappa(p)$ becomes infinite coincides with p_c on most lattices of interest [4].

The connectivity function for two sites x, y is the probability that these two sites belong to the same cluster. For the case of independent percolation one can prove that for $p < p_c$ the connectivity function decays exponentially with the increase of the separation between the two sites with a characteristic length $\xi(p)$ commonly refered to as the correlation length. Similar quantity can be defined for the case of $p > p_c$.

Near the critical density p_c $P_\infty(p)$ vanishes, and both $\kappa(p)$ and $\xi(p)$ diverge:

$$P_\infty(p) \sim |p - p_c|^\beta \text{for } p \searrow p_c \tag{1.1}$$
$$\kappa(p) \sim |p - p_c|^{-\gamma} \text{for } p \nearrow p_c$$
$$\xi(p) \sim |p - p_c|^{-\nu} \text{for } p \to p_c$$

The relations (1.1) define the critical exponents β, γ and ν. Although the full functional dependence of the quantities in (1.1) may depend on the particularities of the percolation model, the critical exponents are the same for all short range correlated percolation models on a given d dimensional lattice. By a short range correlated percolation model we mean a model in which the two point correlation $\langle \eta(x)\eta(y) \rangle$ for the percolation field decays exponentially or as $\frac{1}{|x-y|^a}$ with $a > d$. We will discuss later in this chapter percolation models for which $a < d$, we refer to these as long range correlated percolation models. We will show through some scaling arguments and RG calculation that these long range correlated percolation models define new percolation universality classes that depend on a.

It is notoriously difficult to rigorously calculate the critical exponents defined in (1.1). For Bernoulli site percolation on the $2d$ triangular lattice this has only recently been achieved [30]. For long range correlated percolation models this is an impossible task. However, renormalization group calculations can be used to compute the critical exponents up to a given accuracy [31, 32]. We will use the momentum space renormalization group in Sec. 3.5 and will try to compute β,γ and ν for the long range correlated percolation models up to a two loop expansion.

One can also use Monte Carlo simulations together with a finite size scaling anzatz, and compute the critical exponents in this way. We will do that in Chapter 4 for two particular models possessing long range correlations, the Harmonic Crystal and the Voter model.

The finite size scaling idea is simple [31]. Equations (1.1) correspond to quantities calculated in an infinite system. The question is how the relations above would change if one calculated these quantities in a finite system of linear size L. The answer is

simple:

$$X(L,\xi) = \xi^{\frac{\kappa}{\nu}} f(L/\xi) \tag{1.2}$$

for a quantity X whose infinite size version decays as $|p-p_c|^{-\kappa}$.

3.2 Scaling Analysis of Long Range Correlated Percolation

For the rest of this thesis we study the effects of correlations on the percolation critical properties. In this section we use scaling arguments to show that the introduction of long range correlations drives the percolation model into a new universality class. We follow closely the exposition in [1] where these calculations have been first presented.

If the correlations are short range then we can use the usual Harris criteria to determine if they are relevant or not. According to this criteria the correlations are relevant if $d\nu - 2 < 0$, here ν is the percolation correlation length critical exponent for an independent percolation model. For independent percolation $d\nu - 2 > 0$ for all $d > 0$ so we conclude that short range correlated percolation belongs to the universality class of Bernoulli independent percolation. We confirm this observation for the noisy voter model and the massive harmonic crystal using monte carlo simulation, see Sec. 4.2.4.

Using scaling arguments, a criteria for the releveance of the correlations similar to that of Harris can be derived for the case of long range correlations. Let $\eta(x) = \{1, 0\}$ be our occupation variable, $\langle \eta(x) \rangle = p$ and

$$g_\eta(|x-y|) = \langle \eta(x)\eta(y) \rangle - \langle \eta(x) \rangle \langle \eta(y) \rangle. \tag{2.1}$$

To derive the scaling relations we need the following assumption. For a cubic region Λ containing $|\Lambda|$ sites the largest cluster is of size $\xi_\Lambda \sim |p_c - p_\Lambda|^{-\nu}$, where p_c is the critical density of the infinite system and $p_\Lambda = \frac{1}{V}\sum_{x\in\Lambda} \eta(x)$ is the density of occupied sites inside the cube Λ. To be consistent we require the length L of the cube Λ to satisfy the inequality $L \geq \xi_\Lambda$. In what follows we take $L = \xi_\Lambda$.

Let us calculate the variance Δ of p_Λ

$$\begin{aligned} \Delta^2 \equiv \langle {p_\Lambda}^2 \rangle - \langle p_\Lambda \rangle^2 &= \frac{1}{V^2} \sum_{x,y\in\Lambda} \{ \langle \eta(x)\eta(y) \rangle - \langle \eta(x) \rangle \langle \eta(y) \rangle \} \\ &\sim \frac{1}{\xi^d} \int_0^\xi g_\eta(r) r^{d-1} dr. \end{aligned} \tag{2.2}$$

In (2.2) we have taken $V = \xi^d$ with ξ growing large as $p \to p_c$. A uniform percolation transition is consistent only if $\frac{\Delta^2}{(p-p_c)^2} \to 0$ as $p \to p_c$. After performing the integral in (2.2) one obtains

$$\frac{\Delta^2}{(p-p_c)^2} = \begin{cases} (p_c - p)^{d\nu-2}, & a > d \\ (p_c - p)^{a\nu-2}, & a < d \end{cases} \tag{2.3}$$

For $a > d$ we conclude that a percolation transition with the independent percolation correlation length exponent ν is consistent as mentioned above. For $a < d$ however we see that if $a\nu - 2 < 0$ then we expect a that the correlations are relevant and will change the properites of the percolation transition.

We can push this analysis further and actually identify the new correlation length critical exponent. To do that imagine that $g_\eta(x)$ decays as $\frac{A}{|x|^a} + \frac{B}{|x|^b}$. If $b < a$ then the B term will eventually dominate and we expect the model to have a different critical behavior from the model for which only the A term is present. If however $b > a$ then the A term dominates and the system should belong to the universality class of the model for which only the A term is present. We conclude that $b\nu_{long} - 2 > 0$ if $b > a$ and $b\nu_{long} - 2 < 0$ if $b > a$. If this is to be true for every b then necessarily

$$\nu_{long} = \frac{2}{a} \tag{2.4}$$

This scaling analysis based on a mean field type calculation tells us that we have a continuity of percolation universality classes defined by a. Amazingly the analysis also gives us an exact prediction for the new correlation length critical exponent ν_{long}.

In the Sec. 3.5 we analyze this problem from a field theoretical point of view. We confirm the results of the scaling analysis above and we also obtain estimates for the other critical exponents in terms of a double expansion in $\epsilon = 6 - d$ and $\delta = 4 - a$.

3.3 Field Theory Approaches to Percolation

The relation between Potts model and percolation arises from the random cluster description of the Potts model as discussed in Sec. 2.2. This relation allows one to calculate

the percolation transition critical exponents through the use of renormalization group study of a Hamiltonian description of the Potts model. One needs to first construct a continuum generalization and formulation of the q-state Potts model and then use momentum space RG and finally take the $q \to 1$ limit to calculate the critical exponents associated with the percolation transition.

Such a continuum formulation of the q-state Potts model was introduced in [33], it involves a diagonal traceless tensors $Q_{i,j}$ of dimension q. The Hamiltonian for this model is

$$H = \frac{1}{2}\int d^d x (rTrQ^2 + \sum_{i,j,k} \nabla_i Q_{jk} \nabla_i Q_{jk}) + \int d^d x (wTrQ^3 + u(TrQ^2)^2 + vTrQ^4). \quad (3.1)$$

For percolation the upper critical dimension is 6 and thus the terms of fourth and higher order in $Q_{i,j}$ are irrelevant. To see the relation between this model and the q-state Potts model one needs to introduce and appropriate decomposition of Q for details on this see [33].

One can now use dimensional regularization and renormalization to obtain an expression for the critical exponents in terms of an $\epsilon = 6 - d$ expansion [33]. One can also use Parisi's fixed dimensional renormalziation scheme to calculate directly the critical exponents in say 3 dimensions [34] . We will have more to say about this later.

In [1] Weinrib noticed that analogous relation between the long range correlated percolation problem and a disordered q-state Potts ferromagnet exists. It can be argued that the critical exponents for the correlated percolation problem can be obtained through a mapping of the percolation problem to the $q \to 1$ limit of the q-state Potts model with long range correlated quenched coupling-constant disorder [1]. Weinrib obtains the field theoretic formulation of the disordered q-state Potts model by considering the Hamiltonian in (3.1) with a random "temperature" coefficient $r(x)$. To find the free energy of the disordered q-state Potts model he uses the replica technique. In the end, all of this results into an effective Hamiltonian on which a double expansion in ϵ and δ up to one loop was performed [1].

In this thesis we use another, in my opinion more elegant approach to the percolation problem. It was noticed by Cardy and Grassberger [35] that the statistical

properties of the clusters of independent percolation near a percolation threshold can also be studied using the General Epidemic Process(GEP). GEP is an example of an absorbing state phase transition. For this process a "disease" is spreading through a media of susceptible individuals. The susceptible media becomes infected with rate dependent on the density of the sick and the density of recovered individuals. After a brief time interval the sick recover and are immune after that. The recovered individuals, sometimes referred to as debris when GEP is used to describe the spread of fire for example, stop the spread of the disease locally. The state with zero density of sick individuals is absorbing, i.e. the disease can not spontaneously reappear. The statistical properties of the debris clusters that are left behind after the disease has been extinguished are described by independent percolation [36, 35]. This description of the independent percolation problem allows to probe in addition to the exponents ν, γ and β also the spreading exponent z_s which is connected to the dynamic exponent z of the DIP field theory by the relation $z_s = \frac{2}{z}$ [36, 35]. The shortest path , or chemical distance, between two points on the infinite cluster a distance r apart scales like r^{z_s}, where z_s is the spreading exponent.

We consider a DIP field theory for which the critical control parameter τ is disordered with a quenched correlated disorder that decays for large distances r as r^{-a}. The static properties of the clusters that are left behind after the agent has been extinguished are described by long range correlated percolation. Performing the averaging over the disorder for this dynamical model is easy, we do not need the replica trick [37]. After that we renormalize the resulting field theory using dimensional regularization and minimal subtraction.

The procedure of dimensional regularization and minimal subtraction results in a power series in terms of ϵ and δ for the critical exponents. For independent percolation, the power series now are in terms of ϵ only, such an expansion even only to two loops after a Pade-Borel resummation agrees well for $d \geq 3$ with the values of the critical exponents obtained from simulations [34]. For the minimal distance exponent the agreement is remarkable [32]. One might hope, even if it is not realistic, that such an agreement might hold for the correlated percolation problem when the power series

are in terms of the two parameters ϵ and δ. Higher than one loop double expansion however for such models seem to be difficult. In this thesis we consider the special case $\epsilon = \delta$. For such a model we perform a two loop calculation.

The results from the two loop calculation do not agree well with simulation results, this is not very surprising. The power series for the exponents that one obtains from such an expansion might not even be resummable, and even if it is, the structure of the problem is much more complicated than the one of independent percolation so higher loop calculation might be needed to get comparable result.

Another RG approach for calculating critical exponents from field theories is the fixed dimensional renormalization based on Parisi's "massive" scheme [38]. Such an approach for independent percolation for $d \geq 3$ up to two loops gives quite good agreement with the simulation results [34]. The agreement is better than the one based on the ϵ expansion. Such an approach was used in [39] to calculate the critical exponents for $O(m)$-symmetric Ginzburg-Landau-Wilson model in quenched disorder with power law correlations for $d = 3$ and $2 \leq a \leq 3$. We have tried to do similar calculation for the long range percolation problem for $d = 3$ and a close to 2. However even after Pade-Borel resumation the calculations did not reveal any fixed points other than the pure one. Details of how one performes such a calculation can be found in the Appendix to this Chapter.

The rest of this Chapter is organized as follows. In Sec. 3.4 we present the field theoretic description of the independent DIP model. We also present there a sketch of the renormalization procedure and how one extracts the critical exponents from the RG equations. In section Sec. 3.5 we discuss our generalization of DIP where we introduce the long range correlated quenched randomness. A first order calculation is performed and the new fixed point corresponding to long range percolation is identified. Then we present the results of the two loop calculation for the special case $\epsilon = \delta$. In Sec. 3.6 we present simulation results for the Voter model. In the Appendix to this Chapter we provide some details of the calculations.

3.4 Dynamic Isotropic Percolation

There are two ways to extract an effective field theory functional which after an RG study gives the critical exponents of DIP [32]. One approach is to start from the master equation of the microscopic dynamics of a specific model in the DIP universality class. Representing this in terms of bosonic creation and annihilation operators and using coherent-states one can proceed towards field theory [40]. A second approach is to use phenomenological arguments and write down an effective Langevin equation obeying all the requirements and symmetries of the theory. We can map this equation into a field theory functional [36]. Following this general principle one obtains the following effective action for DIP

$$I\left[s,\hat{s}\right]=\int d^{d}rdt\left\{\hat{s}\left[\partial_{t}+\lambda\left(\tau-\bigtriangledown^{2}\right)+\frac{\lambda g}{2}\left(2S-\hat{s}\right)\right]s\right\} \tag{4.1}$$

where $S(r,t)=\lambda\int_{0}^{t}dt^{'}s(r,t^{'})$ is the density of debris at site r, $s(r,t)$ is the density of infected individuals, τ is the critical control parameter, λ is proportional to the recovery rate, and finally $\hat{s}$ is the response field.

The naive scaling dimensions of the fields and couplings for the DIP action are as follows

$$S\sim\hat{s}\sim\mu^{(d-2)/2}$$
$$s\sim\mu^{(d+2)/2}$$
$$g\sim\mu^{(6-d)/2}$$

where μ is an arbitrary scale of length an time. We see that the upper critical dimension d_c of the theory is 6, that is for $d>6$ the theory is asymptotically free.

In the calculation of the Green's functions of a general field theory ultraviolet divergences arise, also infrared divergences if we are at the critical point. For a renormalizable field theory the divergences can be removed by absorbing them in the bare coupling constants and fields. For the DIP field theory we define renormalized fields

and couplings as follows [32]

$$s_r = Z^{-1/2} s, \quad \hat{s}_r = \hat{Z}^{-1/2} \hat{s}$$
$$u = G_\epsilon g^2 \hat{Z}^3 {Z_u}^{-1} \mu^{-\epsilon}, \quad \lambda_r = (Z\hat{Z})^{1/2} \hat{Z}^{-1} \lambda$$
$$\tau = \hat{Z}^{-1} Z_\tau \tau_r + \tau_c,$$

where, $\epsilon = 6 - d$, $G_\epsilon = \frac{\Gamma(1+\epsilon/2)}{(4\pi)^{d/2}}$. The renormalization constants $Z_{...} = Z_{...}(u, \mu/\Lambda, \epsilon)$ can be chosen in a UV-renormalizable theory in such a way that

$$G^r_{N,\hat{N}}(\{r,t\}, \tau_r, u, \lambda_r, \mu) = \lim_{\Lambda\to\infty} Z^{-N/2} \hat{Z}^{-\hat{N}/2} G(\{r,t\}, \tau, g, \lambda, \Lambda) \tag{4.2}$$

and $G^r_{N,\hat{N}}$ in (4.2) are finite and well defined, here $G(...)$ are the Green's functions of the theory. We have regularized the field theory in (4.2) by introducing a high momentum cutoff Λ. For $d \leq d_c$ the critical theory has IR singularities and for $d \geq d_c$ the theory has UV singularities. Indeed, the problematic UV and IR singularities are linked precisely at $d = d_c$. What is important is that the determination of the Z factors coming from the UV divergence provides information of the critical IR singularities and thus on the critical exponents [32, 41].

In the explicit calculation that we perform we fix $\epsilon > 0$ and take the continuum limit $\Lambda \to \infty$ and we require that the Z factors absorb the ϵ poles. This procedure is called minimal subtraction. Note that in such a calculation τ_c is set to zero. By requiring that as $\epsilon \to 0$ the theory gives finite results we can calculate the exponents as power series in ϵ.

The bare Green's functions are independent of the renormalization scale μ therefore from (4.2) follows the Renormalization Group (RG) equation:

$$\left[\mu\frac{\partial}{\partial\mu} + \xi\lambda_r\frac{\partial}{\partial\lambda_r} + k\tau_r\frac{\partial}{\partial\tau_r} + \beta\frac{\partial}{\partial u} + \frac{1}{2}(N\Upsilon + \hat{N}\hat{\Upsilon})\right] G^r_{N,\hat{N}}(r, t, \tau_r, u, \lambda_r, \mu) = 0 \tag{4.3}$$

where

$$\beta(u) = \mu \left.\frac{\partial u}{\partial\mu}\right|_0 \quad \Upsilon(u) = \mu \left.\frac{\partial \ln Z}{\partial\mu}\right|_0, \quad \hat{\Upsilon}(u) = \mu \left.\frac{\partial \ln \hat{Z}}{\partial\mu}\right|_0$$
$$k(u) = \mu \left.\frac{\partial \ln \tau_r}{\partial\mu}\right|_0 \quad \xi(u) = \mu \left.\frac{\partial \ln \lambda_r}{\partial\mu}\right|_0. \tag{4.4}$$

The partial differential equation (4.3) can be solved employing the method of characteristics. After solving the RG equation and employing dimensional scaling one arrives to an asymptotic form, long distance , long time of the Green's function from which the critical exponents can be obtained [32]. The critical exponents of the percolation problem are given by

$$\frac{\gamma}{\nu} = 2 - \hat{\Upsilon}(u^*)$$
$$\frac{1}{\nu} = 2 - k(u^*)$$
$$z = 2 + \xi(u^*)$$

where u^* is a stable fixed point of the RG, that is $\beta(u^*) = 0$ and $\beta^{'}(u^*) > 0$.

An RG study through an $\epsilon = d - 6$ expansion for DIP results in exponents which agree with the exponents obtained from an ϵ expansion of the q-state Potts model in the $q \to 1$ limit [35].

3.5 Correlated Dynamic Isotropic Percolation

Let us introduce a variation of DIP in which the critical control parameter τ that governs the strength of the infection is itself position dependent variable $\tau + c(r)$, with $c(r)$ some random field.

If we take static Gaussian distributed disorder with correlations $\langle c(r_1), c(r_2)\rangle \sim f\delta(r_1 - r_2)$ and zero average, f the strength of the disorder, and we perform the average, we observe that the scaling dimension of f is $4 - d$. This is an irrelevant perturbation near 6 dimensions so we expect this kind of disorder not to change the critical behavior.

If however we assume Gaussian disorder with correlations $\langle c(r_1)c(r_2)\rangle \sim f\frac{1}{|r_1 - r_2|^a}$ and zero average, then the scaling dimension of f is $4-a$ which is a relevant perturbation for $a < 4$. The explicit form of the functional is

$$I[s, \hat{s}] = \int d^d r dt \left\{ \hat{s} \left[\partial_t + \lambda \left(\tau - \bigtriangledown^2 \right) + \frac{\lambda g}{2} (2S - \hat{s}) \right] s \right\} - \frac{\lambda^2 f}{2} \int dt_1 \int dt_2 \int d^d r_1 \int d^d r_2 \hat{s}(r_1, t_1)\, s(r_1, t_1) \frac{1}{|r_1 - r_2|^a} \hat{s}(r_2, t_2)\, s(r_2, t_2). \tag{5.1}$$

If we are only interested in time independent quantities (emerging as $t \to \infty$) it is convenient to go to the quasi-static limit [32]. Taking the quasi-static limit amounts to switching the fundamental field variable from the agent density s to to the final density of debris $\phi(r) := S(r,\infty) = \lambda \int_0^\infty s(r,t)dt$ that is ultimately left behind by the epidemic and the associated response field $\hat{\phi}(r) = \hat{s}(r,0)$ [32].

The structure of the action allows us directly to let

$$\hat{s}(r,t) \to \hat{\phi}(r), \qquad \phi(r) = \lambda \int_0^\infty s(r,t)dt$$

This results in the quasi-static Hamiltonian:

$$\begin{aligned} H\left[\phi,\hat{\phi}\right] = &\int d^d x \left\{\hat{\phi}\left[\tau - \bigtriangledown^2 + \frac{g}{2}(\phi - \hat{\phi})\right]\right\} \\ &- \frac{1}{2} f \int d^d x_1 \int d^d x_2 \phi(x_1)\hat{\phi}(x) \frac{1}{|x_1 - x_2|^a} \phi(x_2)\hat{\phi}(x_2) \end{aligned} \tag{5.2}$$

In addition to the rules coming from the Hamiltonian above we have to specify that closed propagator loops are not allowed.

It is more convenient to carry the calculations in momentum space. The Fourier transform of the interaction vertex $g(x) \sim x^{-a}$ is $g(k) = v + wk^{a-d}$ for small k [3]. As discussed at the beginning of this section v is irrelevant and will be ignored, $w > 0$. We now absorb w in the definition of f.

Using again the arbitrary inverse length scale μ by inspection we obtain that

$$\hat{\phi} \sim \phi \sim \mu^{d/2}$$
$$g \sim \mu^{\frac{6-d}{2}} \quad f \sim \mu^{4-a}$$

The upper critical dimension is 6 and f is relevant for $a < 4$. The propagator is

$$G(q) = \frac{1}{\tau + q^2} \tag{5.3}$$

and the vertices are given by $U_1 = -U_2 = g$ and $V = \frac{f}{q^{d-a}}$. To extract the divergences we have only to calculate the one particle irreducible diagrams denoted here by Γ. Inspection of the naive divergence of the one particle irreducible diagrams show that they arise only in the diagrams contributing to $\Gamma^{1,1}$, $\Gamma^{1,2} = -\Gamma^{2,1}$ and $\Gamma^{2,2}$. Here the

first index is the number of amputated external $\hat{\phi}$ legs and the second is the number of amputated ϕ legs. The vertex functions are considered as functions of external momenta and we require that $\Gamma^{1,2}(0)$, $\Gamma^{2,2}(0)$, $\Gamma^{1,1}(0)$ and $\frac{d\Gamma^{1,1}}{dp^2}\Big|_{p^2=0}$ are finite. The model is renormalizable by the following scheme

$$\begin{aligned}
\phi_r = \hat{Z}^{-1/2}\phi, \quad \hat{\phi}_r &= \hat{Z}^{-1/2}\hat{\phi}, \\
\tau_r &= Z_\tau^{-1}\hat{Z}\tau, \\
u &= G_\epsilon \mu^{-\epsilon}\hat{Z}^3 Z_u^{-1} g^2, \\
v &= F_\delta \mu^{-\delta}\hat{Z}^2 Z_v^{-1} f.
\end{aligned}$$

where $F_\delta = \frac{G(1+\frac{\delta}{2})\Gamma(\frac{a}{2})}{4\pi^{d/2}\Gamma(\frac{d}{2})}$ and $\delta = 4 - a$. Evaluating to one loop order the divergent diagrams and using minimal subtraction and double expansion, where now we require that the Z factors absorb both ϵ and δ poles, we obtain the following results

$$\begin{aligned}
\hat{Z} &= 1 + \frac{u}{6\epsilon} - \frac{4v}{6\delta}, \\
Z_\tau &= 1 + \frac{u}{\epsilon} - \frac{2v}{\delta}, \\
Z_u &= 1 + \frac{4u}{\epsilon} - \frac{12v}{\delta}, \\
Z_v &= 1 + \frac{2u}{\epsilon} - \frac{4v}{\delta}.
\end{aligned}$$

This gives us

$$\begin{aligned}
\beta(u) &= u(-\epsilon + \frac{7}{2}u - 10v), \\
\beta(v) &= v(-\delta + \frac{5}{3}u - \frac{8}{3}v), \\
k(u,v) &= \frac{5u - 8v}{6}, \\
\bar{\Upsilon}(u,v) &= -\frac{u}{6} + \frac{4v}{6}.
\end{aligned}$$

A nontrivial fixed point, which corresponds to long range correlated percolation is obtained:

$$\begin{aligned}
u^* &= \frac{15\delta - 4\epsilon}{11}, \\
v^* &= \frac{21\delta - 10\epsilon}{44}.
\end{aligned}$$

which finally gives us

$$\frac{1}{\nu} = 2 - \frac{\delta}{2} \qquad (5.4)$$
$$\frac{\gamma}{\nu} = 2 - \frac{\delta - \epsilon}{11}$$

One could carry the stability analysis for the different fixed points and he will arrive at the same conclusion as in [1], that is this calculation confirms the scaling arguments in Sec. 3.2

In contrast to [1] our formulation allows us to compute the spreading exponent as well. In order to do this calculation we have to go back to the dynamical model. Fortunately to extract the dynamical critical exponent we have to only calculate $\Gamma^{1,1}$, as a function of the external momentum q and frequency ω. From the renormalization of the derivative $\frac{\partial \Gamma_{1,1,}}{\partial \omega}\Big|_{q^2=\omega=0}$ we obtain

$$(Z\hat{Z})^{1/2} = 1 + \frac{3u}{4\epsilon} - \frac{2v}{\delta} \qquad (5.5)$$

and from this we conclude that

$$\xi(u^*, v^*) = -\frac{7u^*}{12} + \frac{4v^*}{3} = -\frac{\epsilon}{11} - \frac{7\delta}{44}, \qquad (5.6)$$

and thus

$$z = 2 + \xi(u^*, v^*) = 2 - \frac{\epsilon}{11} - \frac{7\delta}{44}. \qquad (5.7)$$

We are interested in obtaining estimates for the critical exponents for long range correlated percolation for $d \geq 3$. It is quite remarkable that such estimates for independent percolation in $d \geq 3$ coming from an ϵ expansion up to two loops agree well with simulation results [34]. The agreement for the spreading exponent is quite remarkable [32]. Although it might be unrealistic we are curious whether such an agreement might hold for the case of long range correlated percolation. Unfortunately it is seems difficult to carry out a two loop double expansion in ϵ, δ. We note here that we have performed a fixed dimension renormalization for $d = 3$, and a close to 2, which did not result any fixed point other than the pure one even after Pade-Borel resummation was performed, see Sec. 3.8.1.

We have performed a two loop expansion for the case $\epsilon = \delta$, in this case it is just

an expansion in ϵ. Such models arise naturally when the correlation are expressed in terms of the probability that a random walk starting at a given site will hit the origin, this probability for $d \geq 3$ is proportional to $\frac{1}{|x|^{d-2}}$, thus $a = d - 2$. Examples for such models are the Voter Model and the Massles Harmonic crystal in $d \geq 3$ [42]. From the ϵ expansion we obtain

$$\begin{aligned}
Z_u &= 1 + \frac{1}{\epsilon}(4u - 6v) + uv(\frac{69}{4\epsilon} - \frac{39}{\epsilon^2}) + u^2(-\frac{59}{12\epsilon} + \frac{15}{\epsilon^2}) + v^2(-\frac{145}{12\epsilon} + \frac{22}{\epsilon^2}),\\
Z_v &= 1 + \frac{2}{\epsilon}(u - v) + uv(\frac{91}{18\epsilon} - \frac{32}{3\epsilon^2}) + u^2(-\frac{47}{24\epsilon} + \frac{11}{2\epsilon^2}) + v^2(-\frac{91}{36\epsilon} + \frac{10}{3\epsilon^2}),\\
Z &= 1 + \frac{1}{\epsilon}(\frac{u}{6} - \frac{v}{3}) + uv(\frac{71}{144\epsilon} - \frac{3}{4\epsilon^2}) + u^2(-\frac{37}{432\epsilon} + \frac{11}{36\epsilon^2}) + v^2(-\frac{139}{216\epsilon} + \frac{5}{18\epsilon^2}),\\
Z_\tau &= 1 + \frac{1}{\epsilon}(u - v) + uv(\frac{91}{36\epsilon} - \frac{13}{3\epsilon^2}) + u^2(-\frac{47}{48\epsilon} + \frac{9}{4\epsilon^2}) + v^2(-\frac{91}{72\epsilon} + \frac{7}{6\epsilon^2}).
\end{aligned}$$

This gives us

$$\begin{aligned}
\beta_u &= (-\epsilon + \frac{7}{2}u - 5v - \frac{671}{72}u^2 + \frac{757}{24}vu - \frac{731}{36}v^2)u\\
\beta_v &= (-\epsilon + \frac{5}{3}u - \frac{4}{3}v - \frac{193}{54}u^2 + \frac{293}{36}vu - \frac{67}{27}v^2)v
\end{aligned}$$

$$\begin{aligned}
\bar{\Upsilon}(u,v) &= -\frac{1}{6}u + \frac{1}{3}v + \frac{37}{216}u^2 - \frac{71}{72}vu + \frac{139}{108}v^2\\
k(u,v) &= \frac{5}{6}u - \frac{2}{3}v - \frac{193}{108}u^2 + \frac{293}{72}uv - \frac{67}{54}v^2
\end{aligned}$$

We identify a long range stable fixed point:

$$\begin{aligned}
u^* &= \epsilon + \frac{59}{88}\epsilon^2,\\
v^* &= \frac{1}{2}\epsilon + \frac{131}{176}\epsilon^2
\end{aligned}$$

which results in

$$\begin{aligned}
k(u^*, v^*) &= \frac{1}{2}\epsilon, \qquad (5.8)\\
\bar{\Upsilon}(u^*, v^*) &= \frac{3}{22}\epsilon^2
\end{aligned}$$

From the dynamical part of the calculation we obtain

$$\begin{aligned}
(Z\bar{Z})^{\frac{1}{2}} = 1 &+ \frac{1}{\epsilon}(\frac{3}{4}u - \frac{227}{384}u^2 + \frac{569}{288}vu - v - \frac{91}{72}v^2 + \frac{1}{8}uv\log(2) + \frac{5}{32}\log(2)u^2 - \frac{9}{64}\log(3)u^2)\\
&+ \frac{1}{\epsilon^2}(\frac{51}{32}u^2 - \frac{83}{24}uv + \frac{7}{6}v^2). \qquad (5.9)
\end{aligned}$$

This gives us

$$\xi(u,v) = -\frac{7}{12}u + \frac{2}{3}v + (\frac{1747}{1728} - \frac{5}{16}\log(2) + \frac{9}{32}\log(3))u^2 - (\frac{427}{144} + \frac{1}{4}\log(2))uv + \frac{67}{54}v^2.$$

For the dynamic exponent, and consequently the spreading exponent, for the long range fixed point we finally obtain

$$\begin{aligned} z &= 2 - \frac{1}{4}\epsilon + (-\frac{119}{2112} - \frac{7}{6}\log(2) + \frac{9}{32}\log(3))\epsilon^2 \\ z_s &= \frac{2}{z} = 1 + \frac{1}{8}\epsilon + (\frac{185}{4224} + \frac{7}{32}\log(2) - \frac{9}{64}\log(3))\epsilon^2 \end{aligned} \tag{5.10}$$

To summarize, the two loop expansion gives for the correlation length critical exponent $\nu = \frac{2}{a}$. For the ratio of critical exponents $\frac{\gamma}{\nu}$ we obtain to one loop 2, compare to the result of 1.8 in [42], but there is a big correction of $-\frac{3}{22}\epsilon^2$ coming from the two loops. From a Pade-Borel resummation of the series for z_s we obtain $z_s \approx 1.6$ for $d = 3$. In the next section we report on simulation results for z_s for the Voter model percolation problem on $\mathbb{Z}^3$ [42].

3.6 Spreading exponent for the Voter Model percolation

To obtain the spreading exponent for independent percolation one uses the Leath algorithm. This corresponds to growing a cluster from a single seed [43]. One could stop the growth after a certain number of "steps" or after the cluster hits a certain boundary, the first is more natural. For the Voter model percolation problem this approach is not possible, we can not grow single clusters since the occupation probabilities are not independent. For a description of the Voter model see Chapter 4

We use the algorithm introduced in Chapter 4 to simulate the Voter model. We pick a site and we decide that it is going to be occupied, this is our seed. Then we run our algorithm for a cube that is centered at that site but in addition to the rules detailed in Chapter 4 when a random walker hits the center we freeze it and assign all of it ancestors occupied in the percolation problem

We simulate the Voter model at its critical density $p = 0.1$, see Chapter 4, the results are presented in Fig. 3.1. In fact not much fluctuation in the results for z_s is observed for $p \in [0.9, 0.11]$. We conclude that $z_s \approx 1.32$. This is smaller than the exponent

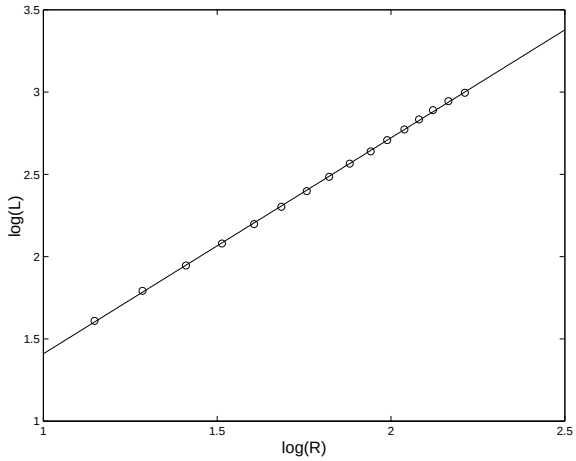

Figure 3.1: Plot of $\log(R)$ versus $\log(L)$ for the 3d voter model at $p = 0.1$. The slope of the straight line gives $z_s \approx 1.32$

of independent percolation which is $z_s \approx 1.37$ [43]. This result clearly does not agree with our ϵ expansion result.

3.7 Conclusion

We have investigated the field theory of quenched correlated disordered DIP with disorder correlations that decay at large distances r as r^{-a}. We have identified a long range stable fixed point in a one loop double expansion in $\epsilon = 6 - d$ and $\delta = 4 - a$. Our results agree with the results obtained in [1] using a different representation of the problem as well as different RG scheme.

For the special case $\epsilon = \delta$ we have performed an expansion to 2nd order in ϵ. For the correlation length critical exponent we have obtained $\nu = \frac{2}{a}$, for the ratio of critical exponents $\frac{\gamma}{\nu}$ the results is $2 - \frac{3}{22}\epsilon^2$ and for the spreading exponent z_s the result is $z_s = 1 + \frac{1}{8}\epsilon + (\frac{185}{4224} + \frac{7}{32}\log(2) - \frac{9}{64}\log(3))\epsilon^2$. For $d = 3$ after a Pade-Borel resumation of the series we obtained $z_s \approx 1.6$. From a simulation of the Voter model in 3d we have obtained $z_s \approx 1.32$.

We have also performed a fixed dimensional renormalization at $d = 3$ and a close to 2, and we did not find any fixed points other than the pure one. It would be interesting to perform such a calculation in the case of $d = 5$ and $a = 3$ to see if a stable long

range fixed point will appear and how would the results compare with the result of the ϵ expansion.

3.8 Appendix

For the quasi-static limit the propagator and interaction vertices are

Propagator

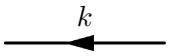

$\frac{1}{k^2+\tau}$

Interaction vertices

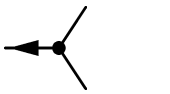

$-g$

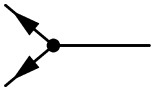

g

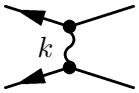

$\frac{f}{k^{d-a}}$

To one loop in the quasi-static limit the diagrams that contribute to the different $\Gamma's$ are listed below.

$\Gamma^{1,1}$ 

$\Gamma^{1,2}$ 

$\Gamma^{2,2}$ 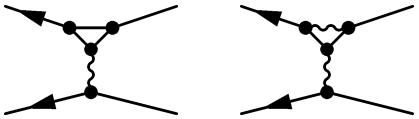

For the dynamical theory the propagator and vertices are

Propagator

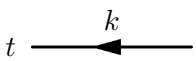

$\theta(t)\exp(-\lambda(\tau+k^2)t)$

Interaction vertices

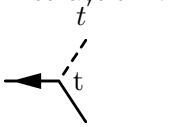

$-\lambda^2 g\theta(t-t^{'})$

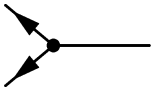

λg

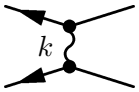

$\frac{\lambda^2 f}{k^{d-a}}$

Notice the appearance of a time delocalized vertex [36]. For the two loop calculation we consider all topologically different diagrams that can be obtained with our vertices and propagator, we discard all diagrams which contain closed propagator loops.

The values of the diagrams that appear in our two loop calculation could be represented as sums of three types of integrals, or their derivatives with respect to the parameters, a,b and c.

$$I_1(a,b,c) = \int \frac{d^d k_1 d^d k_2}{(a+k_1^2)(b+k_2^2)(c+(k_1+k_2)^2)} \tag{8.1}$$
$$I_2(a,b,c) = \int \frac{d^d k_1 d^d k_2}{(a+k_1^2)(b+k_2^2)(c+k_1^2+(k_1+k_2)^2)}$$
$$I_3(a,b,c) = \int \frac{d^d k_1 d^d k_2}{(a+k_1^2)(b+k_2^2)(c+k_1^2+k_2^2+(k_1+k_2)^2)}$$

Only integrals of type I_1 appear in the calculation of the quasi static limit, while all types of integrals appear in the calculation of the dynamic exponent. In our calculation the integral I_1 and its derivatives are evaluated at the point $a=b=c=1$ or $a=0$,$b=c=1$, integral I_2 and its derivatives are evaluated at the point $a=b=1, c=2$ or $a=0, b=1, c=2$ and integral I_3 and its derivatives are evaluated at the point $a=b=1, c=3$ or $a=0, b=1, c=3$. The dimensional regularized form of the

integrals I_1 and I_3 can be found in the literature [44].

$$
\begin{aligned}
I_1(a,b,c) &= \frac{1}{6\epsilon}G_\epsilon^2\Big(\left(\frac{1}{\epsilon}+\frac{25}{12}\right)\left(a^{3-\epsilon}+b^{3-\epsilon}+c^{3-\epsilon}\right) \\
&\quad -\left(\frac{3}{\epsilon}+\frac{21}{4}\right)\left(a^{2-\epsilon}(b+c)+b^{2-\epsilon}(a+c)+c^{2-\epsilon}(a+b)\right)-3abc\Big) \\
I_3(a,b,c) &= G_\epsilon^2\Big(\frac{1}{\epsilon^2}\Big(\frac{5}{24}(a^{3-\epsilon}+b^{3-\epsilon})-\frac{1}{4}(a^{2-\epsilon}b+b^{2-\epsilon}a)-\frac{1}{8}(a^{2-\epsilon}+b^{2-\epsilon})c\Big) \\
&\quad +\frac{1}{\epsilon}\Big(\Big(\frac{143}{288}-\frac{9}{16}\log\Big(\frac{4}{3}\Big)\Big)(a^3+b^3)+\Big(\frac{1}{12}\log\Big(\frac{4}{3}\Big)-\frac{1}{36}\Big)c^3 \\
&\quad -\Big(\frac{1}{16}+\frac{9}{8}\log\Big(\frac{4}{3}\Big)\Big)(a^2b+b^2a)+\Big(\frac{1}{8}-\frac{1}{2}\log\Big(\frac{4}{3}\Big)\Big)c^2(a+b) \\
&\quad +\Big(\frac{15}{16}\log\Big(\frac{4}{3}\Big)\Big)c(a^2+b^2)+\Big(\frac{3}{2}\log\Big(\frac{4}{3}\Big)-\frac{1}{2}\Big)abc\Big)\Big)
\end{aligned}
\tag{8.2}
$$

For our calculation we only need an expression of the first derivative of $I_2(a,b,c)$ with respect to c for that we have obtained:

$$
\begin{aligned}
-\frac{\partial I_2(a,b,c)}{\partial c} &= G_\epsilon^2\Big(\frac{1}{\epsilon^2}\Big(\frac{1}{8}a^2+\frac{1}{2}b^2\Big)+\frac{1}{\epsilon}\Big(-\frac{1}{8}\log(2)a^2 \\
&\quad +\frac{9}{8}b^2+\log(2)bc-\frac{1}{8}a^2\log(a)-\log(2)b^2-\frac{1}{4}\log(2)c^2 \\
&\quad -\frac{1}{2}b^2\log(b)+\frac{9}{32}a^2+\frac{1}{4}c^2-\frac{1}{2}\log(2)ab+\frac{1}{2}\log(2)ac+\frac{1}{4}ac-\frac{1}{2}bc\Big)\Big)
\end{aligned}
\tag{8.3}
$$

3.8.1 Fixed Dimensional Renormalization

One way to calculate the critical exponents is the fixed dimensional Parisi's massive scheme [38]. Such a method was used to calculate the critical exponents for independent percolation up to second order in [34]. For our field theory for $d = 3$ there are no divergencies all integrals are finite for a non-zero mass $\tau^{\frac{1}{2}}$. However a perturbative expansion in terms of the bare dimensionless coupling constant to study the critical properties of the systems does not work since the perturbative coupling constant diverges as we approach the critical region. To remedy this, one has to renormalize the parameters and obtain an expansion in terms of the renormalized dimensionless coupling constants. The renormalized mass in this case corresponds to the inverse of the correlation length and thus vanishes as we approach the critical region. In this case if there is a non-trivial fixed point the renormalized coupling constants stay finite and non-zero.

For the quasi-static theory the normalization renormalization conditions are.

$$\begin{aligned}
\Gamma_r^{1,1,0}(\mathbf{p},\tau,g,f)\big|_{\mathbf{p}=0} &= \tau_r,\\
\left.\frac{\partial\Gamma_r^{1,1,0}(\mathbf{p},\omega,\tau,g,f)}{\partial\mathbf{p}^2}\right|_{\mathbf{p}=0} &= 1,\\
\Gamma_r^{2,1,0}(\mathbf{p},\tau,g,f)\big|_{\mathbf{p}=0} &= \tau_r^{\frac{6-d}{4}} g_r,\\
\Gamma_r^{2,2,0}(\mathbf{p},\tau,g,f)\big|_{\mathbf{p}=0} &= \tau_r^{\frac{4-a}{2}} f_r,\\
\Gamma_r^{1,1,1}(\mathbf{p},\tau,g,f)\big|_{\mathbf{p}=0} &= 1.
\end{aligned}$$

Here Γ_r are the renormalized vertex functions computed in terms of the renormalized field and square field ϕ_r and ϕ_r^2, the third subscript corresponds to ϕ^2 insertions, f_r and g_r are the dimensionless renormalized coupling constants and τ_r is the renormalized "square mass". All these are defined as:

$$\begin{aligned}
\phi = \sqrt{Z_\phi}\phi_r \quad &(\text{same for } \hat{\phi})\\
\phi^2 &= Z_{\phi^2}\phi_r^2,\\
g &= \frac{Z_g}{Z_\phi^{3/2}} g_r,\\
f &= \frac{Z_f}{Z_\phi^2} f_r.
\end{aligned}$$

One can obtain the values of the renormalization factors $Z_{\dots}$ and coupling constants as follows

$$\begin{aligned}
Z_\phi &= \left(\left.\frac{d}{dp^2}\Gamma_r^{1,1,0}(\mathbf{p},\tau,g,f)\right|_{\mathbf{p}=\omega=0}\right)^{-1},\\
Z_{\phi^2} &= \left(\Gamma_r^{1,1,1}(\mathbf{p},\tau,g,f)\big|_{\mathbf{p}=\omega=0}\right)^{-1},\\
\tau_r &= \frac{\left.\Gamma_r^{(1,1,0)}(\mathbf{p},\tau,g,f)\right|_{\mathbf{p}=\omega=0}}{\frac{d}{dp^2}\Gamma^{(1+1,0)}},\\
g_r &= \frac{\left.\Gamma_r^{2,1,0}(\mathbf{p},\tau,g,f)\right|_{\mathbf{p}=\omega=0}}{\tau_r^{\frac{6-d}{4}}},\\
f_r &= \frac{\left.\Gamma_r^{2,2,0}(\mathbf{p},\tau,g,f)\right|_{\mathbf{p}=\omega=0}}{\tau_r^{\frac{4-a}{2}}}.
\end{aligned}$$

What we have so far is series of the renormalized coupling constants and "square mass" in terms of the bare ones, when we do the actual calculation we have to invert these series and we do this as follows

$$\beta(g_r) = \mathcal{D}[g_r] = \mathcal{D}[g]\frac{\partial g_r}{\partial g},$$
$$\eta(g_r) = \mathcal{D}[\log Z_\phi] = \mathcal{D}[g]\frac{\partial \log Z_\phi}{\partial g},$$
$$\eta_2(g_r) = \mathcal{D}[\log Z_{\phi^2}] = \mathcal{D}[g]\frac{\partial \log Z_{\phi^2}}{\partial g},$$

where

$$\mathcal{D}[g] = -g(1 - \frac{g}{2}\frac{\partial \log \frac{\tau_r}{\tau}}{\partial g}),$$

η and η_2 give the critical exponents as $\nu = (2 + \eta_2 - \eta)^{-1}$ and $\frac{\gamma}{\nu} = 2 - \eta$.

If we want to calculate the critical exponent z we need an additional renormalization condition

$$\frac{\partial \Gamma_r^{1,1,0}(\mathbf{p}, \omega, \tau, g, f)\Big|_{\mathbf{p}=\omega=0}}{\partial(-i\omega)} = \frac{1}{\lambda_r} \tag{8.4}$$

We introduce a new renormalization factor Z_λ and define η_λ analogously, $z = 2 + \eta_\lambda$.

After one obtains the series for the β function and the critical exponents one performs a resumation. This is usually more appropriate when higher order calculation has been performed, like the 6 loop calculation for the Ising model critical exponents in $3d$ in [45].

These type of resumations are done as follows

$$\sum c_k x^{2k+1} = x \sum c_k (x^2)^k \frac{1}{k!} \int_0^\infty e^{-t} t^u du = \int_0^\infty \sum x e^{-u} \frac{c_k (x^2 u)^k}{k!} du = \int_0^\infty x e^{-u} F(x^2 u) du.$$

We then use a Pade-Borel approximation for F, in our case since we only go to second order we look for an approximate of the form $F(y) = \frac{a_0 + a_1 y}{1 + b_1 y}$.

For independent percolation $f = 0$ this approach gives good results. Before resummation there is no fixed point for the beta function, but after resumation one

miraculously obtains a fixed point and the values of the exponents that are obtained are comparable to simulation results.

For the long range correlated percolation the power series are in terms of two variables and one thus has to apply resumation of series of two variables. This is done analogously to the one variable case.

$$f(u,v) = \sum c_{i,j} u^i v^j = \int_0^\infty e^{-t} F(ut, vt) dt$$

where $F(x,y) = \sum_{i,j} \frac{c_{i,j}}{(i+j)!} x^j y^j$ and again a Pade approximation is applied to this expression. Unfortunately such an approach did not give us any fixed points so we had to resort to dimensional regulraization and calculation of the exponents within this approach as detailed in Sec. 3.5.

3.8.2 Calculation of Integrals

Here we detail how we obtained the result in (8.3); the approach was inspired by [46].

$$-\frac{\partial I_2(a,b,c)}{\partial c} = \int\int \frac{1}{(a+k_1^2)(b+k_2^2)(c+k_2^2+(k_1+k_2)^2)^2} d^d k_1 d^d k_2$$

$$= \int_0^1 dy \int_0^{1-y} dx (1-x-y^2)^{\frac{\epsilon}{2}-3} \{(1-y-x)(c+y(a-c)+x(b-c))^{2-\epsilon} \Gamma(4-d)(2\pi)^d\}$$

define

$$h_{abc} = c + y(a-c),$$
$$w = 1 - y^2,$$
$$k_{abc} = b + y(a-b),$$
$$z = y - y^2.$$

Then we have

$$-\frac{\partial I_2(a,b,c)}{\partial c} = \int_0^1 dy \frac{\Gamma(4-d)}{2-\frac{\epsilon}{2}} [- h_{abc}^{2-\epsilon}(1-y) w^{\frac{\epsilon}{2}-2} +$$
$$\left(-\frac{(2-\epsilon)(b-c)}{\frac{\epsilon}{2}-1}(1-y) h_{abc}^{1-\epsilon} w^{\frac{\epsilon}{2}} - \frac{1}{\frac{\epsilon}{2}-1} k_{abc}^{2-\epsilon} z^{\frac{\epsilon}{2}-1} + \frac{1}{\frac{\epsilon}{2}-1} h_{abc}^{2-\epsilon} w^{\frac{\epsilon}{2}-1} \right) +$$
$$\frac{(2-\epsilon)(b-c)}{\frac{\epsilon}{2}-1} \left(-\frac{(1-\epsilon)(b-c)}{\frac{\epsilon}{2}(1-y)} h_{abc}^{-\epsilon}(w^{\frac{\epsilon}{2}}-1) - \frac{1}{\frac{\epsilon}{2}} k_{abc}^{1-\epsilon}(z^{\frac{\epsilon}{2}}-1) + \frac{1}{\frac{\epsilon}{2}} h_{abc}^{1-\epsilon}(w^{\frac{\epsilon}{2}}-1) \right) -$$
$$\frac{1}{\frac{\epsilon}{2}-1} \left(\frac{(2-\epsilon)(b-c)}{\frac{\epsilon}{2}} k_{abc}^{1-\epsilon}(z^{\frac{\epsilon}{2}}-1) - \frac{(2-\epsilon)(b-c)}{\frac{\epsilon}{2}} h_{abc}^{1-\epsilon}(w^{\frac{\epsilon}{2}}-1) \right)]$$

We want to identify the divergences in this expression as $\epsilon \to 0$. To accomplish that one has to extract the divergences in following type of integrals

$$I_1 = \int_0^1 f(x) x^{\frac{\epsilon}{2}-1}(1-x)^{\frac{\epsilon}{2}-1} dx \tag{8.5}$$
$$I_2 = \int_0^1 f(x)(1-x)^{\frac{\epsilon}{2}-2} dx$$

here $f(x)$ is assumed to be regular function for $x \in [0,1]$.

To calculate I_1 in (8.5 we can split it as follows

$$I_1 = \int_0^{\frac{1}{2}} f(x) x^{\frac{\epsilon}{2}-1}(1-x)^{\frac{\epsilon}{2}-1} dx + \int_{\frac{1}{2}}^1 f(x) x^{\frac{\epsilon}{2}-1}(1-x)^{\frac{\epsilon}{2}-1} dx \tag{8.6}$$

We can deal with the two terms separately.

$$\int_0^{\frac{1}{2}} g(x) x^{\frac{\epsilon}{2}-1} = \int_0^{\frac{1}{2}} \frac{g(x)}{\frac{\epsilon}{2}} d(x^{\frac{\epsilon}{2}}) = \tag{8.7}$$
$$\left. \frac{g(x) x^{\frac{\epsilon}{2}}}{\frac{\epsilon}{2}} \right|_0^{\frac{1}{2}} - \int_0^{\frac{1}{2}} \frac{g(x)}{\frac{\epsilon}{2}} x^{\frac{\epsilon}{2}} dx$$

but as $\epsilon \to 0$, $x^{\frac{\epsilon}{2}} \to 1 + \frac{\epsilon}{2}\log(x)$, substituting this in (8.7) and simplifying the expression one finally obtains

$$\int_0^{\frac{1}{2}} g(x) x^{\frac{\epsilon}{2}-1} = \frac{g(0)}{\frac{\epsilon}{2}} + g\left(\frac{1}{2}\right)\log\left(\frac{1}{2}\right) - \int_0^{\frac{1}{2}} g^{'}(x)\log(x) dx. \tag{8.8}$$

Analogously one can derive an expression for the second integral in the sum in (8.7). For the second integral in (8.5) after similar manipulations one obtains

$$I_2 = -f(0) - \frac{f^{'}(1)}{\frac{\epsilon}{2}} - f^{'}(1) - \int_0^1 f^{''}(x)\log(1-x) dx \tag{8.9}$$

Collecting everything together one obtains (8.3).

3.8.3 Example Calculations

Here we present some examples from the two loop calculation. First we give an example from the quasi-static calculation.

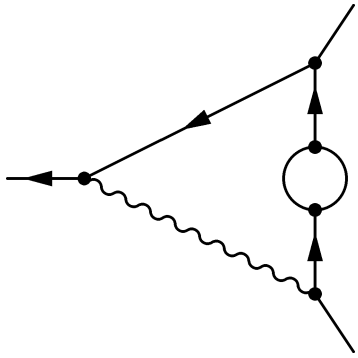

(8.10)

Diagram 8.10 contributes to the calculation of $\Gamma^{1,2}$, we are taking all external momenta to be equal to 0. The integral that we need to calculate is (remember here we are only interested in the case $d-a=2$)

$$\mathcal{I}=\int\int\frac{d^dk_1d^dk_2}{(1+k_1^2)^3(1+(k_1+k_2)^2)(1+k_2^2)(k_1^2)}. \tag{8.11}$$

We represent this integral as

$$\begin{aligned}\mathcal{I}=&\int\int\frac{d^dk_1d^dk_2}{k_1^2(1+(k_1+k_2)^2)(1+k_2^2)}\\&-\int\int\frac{d^dk_1d^dk_2}{(1+k_1^2)(1+(k_1+k_2)^2)(1+k_2^2)}\\&-\int\int\frac{d^dk_1d^dk_2}{(1+k_1^2)^2(1+(k_1+k_2)^2)(1+k_2^2)}\\&-\int\int\frac{d^dk_1d^dk_2}{(1+k_1^2)^3(1+(k_1+k_2)^2)(1+k_2^2)}.\end{aligned}$$

In terms of the integrals in (8.1) we have

$$\mathcal{I}=I_1(0,1,1)-I_1(1,1,1)+\frac{\partial I_1}{\partial a}(1,1,1)-\frac{1}{2}\frac{\partial^2 I_1}{\partial a^2}(1,1,1). \tag{8.12}$$

For the fixed dimensional renormalisation in $3d$ then we have simplified all integrals into integrals of two variables. For the integral associated with diagram 8.10 we have the following expression

$$\mathcal{I}=4\pi^2\int_0^\infty\int_0^\infty\frac{k_1dk_1k_2dk_2}{(1+k_1^2)^3(1+k_2^2)(k_1^2)^{\frac{3-a}{2}}}\log\left(\frac{1+(k_1+k_2)^2}{1+(k_1-k_2)^2}\right). \tag{8.13}$$

We evaluated these type of integrals using Monte Carlo technique.

Now we detail a calculation of a diagram involved in the calculation of the dynamical exponent z.

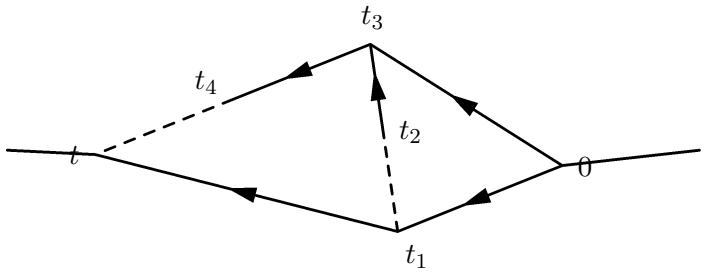

(8.14)

Diagram 8.14 contributes to the calculation of $\Gamma^{1,1}$. Here we are taking the external momentum to be zero. The integral that we need to calculate is

$$\mathcal{I}(t) = \int\int\int\int\int\int e^{-\lambda(\tau+k_1^2)t_3} e^{-\lambda(\tau+k_1^2)t_1} e^{-\lambda(\tau+k_2^2)(t_2-t_1)}$$
$$e^{-\lambda(\tau+(k_1+k_2)^2)(t_4-t_3)} e^{-\lambda(\tau+(k_1+k_2)^2)(t-t_1)} d^dk_1 d^dk_2 dt_1 dt_2 dt_3 dt_4.$$

The time integration in Eq. 3.8.3 is restricted to the region $t > t_4 > t_3 > t_2 > t_1 > 0$. The result after the time integration and a Fourier transform to go from the time variable t into the frequency ω is

$$\mathcal{I}(\omega) = \int\int \frac{1}{(i\omega+2\lambda(\tau+(k_1+k_2)^2))(i\omega+2\lambda(\tau+k_1^2))(i\omega+3\lambda\tau+\lambda k_1^2+\lambda k_2^2+\lambda(k_1+k_2)^2)} d^dk_1 d^dk_2$$
$$-\int\int \frac{1}{(i\omega+2\lambda(\tau+k_1^2))(i\omega+2\lambda(\tau+(k_1+k_2)^2))(i\omega+3\lambda\tau+\lambda k_1^2+\lambda k_2^2+\lambda(k_1+k_2)^2)} d^dk_1 d^dk_2$$
$$-\int\int \frac{1}{(i\omega+2\lambda(\tau+k_1^2))(i\omega+2\lambda(\tau+(k_1+k_2)^2))(i\omega+2\lambda\tau+\lambda k_1^2+\lambda(k_1+k_2)^2)} d^dk_1 d^dk_2$$
$$+\int\int \frac{1}{(i\omega+2\lambda(\tau+k_1^2))(i\omega+\lambda(\tau+(k_1+k_2)^2))(i\omega+2\lambda\tau+\lambda k_1^2+\lambda(k_1+k_2)^2)} d^dk_1 d^dk_2$$

One then has to take a derivative with respect to $i\omega$ and represent this as a sum of the integrals (8.1) or their derivatives as we did in (8.12). When we do the fixed dimensional calculation we first take a derivative with respect to $i\omega$ of $\mathcal{I}$ and then simplify all the resulting integrals in terms of an integral of two variables as in (8.13).

Chapter 4

The Voter Model and The Harmonic Crystal

In this chapter we study the percolation transition in three dimensions for two systems in which the long range correlations arise naturally from the microscopic dynamics: the massless harmonic crystal and the voter model on $\mathbb{Z}^3$. Both of these systems are known rigorously have pair correlations decaying as r^{-1}. They also have other similarities but are intrisicaly quite different. The existence and nature of the percolation transition in these systems is of interest in their own right. Using Monte Carlo simulations and finite size scaling we find the p_c for both models. We also find that both models have the same critical exponents as expected from the WH predictions of a long range percolation universality class.

For the massless harmonic crystal in $\mathbb{Z}^d$ we define site x to be occupied if the scalar displacement field $\phi(x)$ is greater than some preassigned value h and empty if $\phi(x) < h$. Percolation then corresponds to the existence of an infinite level set contour for $\phi(x) < h$. The existence of percolation threshold, i.e. $0 < p_c < 1$, was proven by Bricmont, Lebowitz and Maes [5] for $d = 3$. There are however no previous calculations (known to us) concerning the actual value of p_c or of the critical exponents for this system. One expects intuitively that the p_c will be smaller than the p_c for independent percolation, c.f. [47], but we know of no proof for this. Similarly a proof that $p_c > 0$ for the harmonic crystal in $d > 3$, or for the an-harmonic crystal in $d \geq 3$ is still an open problem [6]. For $d \leq 2$, $\phi(x)$ is for any h, either plus or minus infinity, with probability 1, when the size of the system goes to infinity. Thus either all sites are occupied or all sites are empty.

The voter model, often used for modeling various sociological and biological phenomena , is a lattice system in which a site x is occupied or empty according to whether

the "voter" living there belongs to party A or B. Voters change their party affiliations according to a well defined stochastic dynamics [11]. The stationary state of this model is not known explicitly but many of its properties are known exactly. In particular it has many features in common with the harmonic crystal. Like the harmonic crystal, the stationary state of the voter model is trivial in $d \leq 2$; all sites occupied or all sites empty. On the other hand any p is possible on $\mathbb{Z}^d$ for $d \geq 3$, where the truncated pair correlation decays, as it does for the harmonic crystal, like r^{-1}. No proof of the existence of a $p_c > 0$ is known for this system, i.e. the system could in principle percolate for arbitrary small p. For examples of systems where $p_c \leq \epsilon$ for any $\epsilon > 0$ see [12].

The outline of the rest of this chapter is as follows. In section 4.1 we present the simulation methods and results the massless harmonic crystal. In particular we find $p_c = 0.16 \pm 0.01$. In section 4.2 we study the voter model. We present a new efficient algorithm for simulating this model and report the results from its implementation. We find in particular that $p_c = 0.10 \pm 0.01$ compared with a $p_c \cong 0.16$ obtained in [48] using a less reliable method. We conclude the paper with a brief discussion of some open problems. In the Appendix we justify our simulation algorithm and also provide details of how one could calculate the correlations in the harmonic crystal percolation field and the voter model.

4.1 The Harmonic Crystal

4.1.1 Formulation

Let $x \in \mathbb{Z}^d$ designate the sites of a d-dimensional simple cubic lattice and $\phi(x)$ be the scalar displacement field at site x. The interaction potential in a box Λ with specified boundary conditions (b.c.), e.g. $\phi(x) = 0$ for x on the boundary of Λ, has the form

$$U = \frac{1}{2}J \sum_{<x,y>} (\phi(x) - \phi(y))^2 + \frac{1}{2}M^2 \sum \phi(x)^2 \equiv \frac{1}{2} \sum_{x,y} \phi(x) C^{-1}(x,y) \phi(y) \qquad (1.1)$$

where $J > 0$ and $M \geq 0$, $< x, y >$ indicates nearest neighbor pairs, $|x - y| = 1$, on $\mathbb{Z}^d$. The sum is over all sites in Λ with the specified b.c. The Gibbs equilibrium distribution of the $\{\phi(x)\}$ at a temperature β^{-1}, $\mu_\Lambda^M(\{\phi(x)\}) = Z_{M,\Lambda}^{-1} = e^{-\beta U}$ is then Gaussian with

a covariance matrix $\beta\mathbf{C}$ which is well defined for $M > 0$.

The infinite volume limit Gibbs measure μ^M obtained when $\Lambda \nearrow \mathbb{Z}^d$ is, for $M > 0$, translation invariant, with $\langle\phi(x)\rangle = 0$ and is independent of the boundary conditions [49]. When $M \to 0$, μ^M does not exist for $d \leq 2$ [49]. This is due to the fact that the fluctuations of the field, e.g $\langle\phi(x)^2\rangle$, become unbounded for these dimensions. However, for $d \geq 3$ the Gibbs measure μ obtained as the limit of μ_M when $M \to 0$ is well defined. (It is the same as the infinite volume limit of the measure in a box with $M = 0$ and prescribed boundary values $\phi(x) = 0$). In this limit the pair correlations between different sites have the long distance behavior $\frac{1}{r^{d-2}}$, $r = |x - y|$, for $d > 2$ [49].

Following [5] we define the occupation variable $\rho_h(x)$

$$\rho_h(x) = \begin{cases} 1 & \text{if } \phi(x) \geq h \\ 0 & \text{if } \phi(x) < h \end{cases} \tag{1.2}$$

and let $p = \langle\rho_h(x)\rangle_{\mu^M}$, where the average is over the Gibbs measure μ^M. We can also define a new measure $\hat{\mu}^M$ on the occupation variables $\rho_h(x)$=0,1 by a projection of μ^M. All expectations involving a function of the occupation variables can be computed directly from $\hat{\mu}^M$. The correlations between the occupation variables have the same asymptotic decay properties as those of the field variables ϕ,

$$\langle\rho_h(x)\rho_h(y)\rangle_{\hat{\mu}^M} - p^2 \sim \frac{e^{-|x-y|/\xi_M}}{|x-y|^{d-2}} \quad \text{for } d > 2 \tag{1.3}$$

where $\xi_M \sim M^{-1}$ and the averages are with respect to $\hat{\mu}^M$(or μ^M). In the limit $M \to 0$ the measure $\hat{\mu}$ has a pair correlation that decays like r^{2-d} for $d > 2$. We note that $\hat{\mu}$ is not Gibbsian for any summable potential, c.f [50].

4.1.2 Results

Simulating the harmonic crystal on finite lattices is easy, the elements in a discrete Fourier transform of a harmonic crystal are independently distributed Gaussian random variables with easily computed variances [51]. We consider the system on a lattice with periodic boundary conditions and exclude the zero mode. This is essentially equivalent

to fixing $\langle\phi\rangle = 0$.

There are many methods for obtaining the percolation threshold using data obtained from simulations on finite systems [31]. We used the method employed in [52, 48]. For a cube of linear size L let

$$\Gamma_L = \langle \sum_j j^2 n_j \rangle \tag{1.4}$$

where n_j is the number of clusters of j sites, defined by the occupation variables $\rho_h(x)$, and the average is taken over a large number of samples obtained from simulation of the model. We calculate Γ_L for different sizes L and concentration of occupied sites p defined as in (1.2).

One expects [31, 52, 53] that for large L,and $(p_c - p) \ll 1$, Γ_L should have a finite size scaling form,

$$L^{-d}\Gamma_L \sim L^{\frac{\gamma}{\nu}} F(L^{\frac{1}{\nu}}(p - p_c)) + \text{corrections to scaling}, \tag{1.5}$$

where γ is the critical exponent for the divergence as $p \nearrow p_c$ of the second moment of the cluster size distribution, defined as the limit $L \to \infty$ of $\frac{\Gamma_L}{L^d}$. Corrections to scaling should go to zero for $L \to \infty$.

For $p > p_c$, for an infinite system the second moment of the cluster size distribution can be defined by excluding the infinite cluster. This diverges with a critical exponent $\gamma^{'}$ for $p \searrow p_c$. The finite system analog is $\frac{\Gamma_L^{'}}{L^d}$ which is defined similarly to $\frac{\Gamma_L}{L^d}$ but not including the spanning cluster. $\Gamma_L^{'}$ scales as

$$L^{-d}\Gamma_L^{'} \sim L^{\frac{\gamma^{'}}{\nu}} F^{'}(L^{\frac{1}{\nu}}(p - p_c)) + \text{corrections to scaling}. \tag{1.6}$$

It is believed that $\gamma^{'} = \gamma$.

According to finite size scaling theory the number of sites in the largest cluster in a finite system of linear size L, $P_L(p)$, scales for $|p - p_c| \ll 1$ as

$$P_L(p) \sim L^{d-\frac{\beta}{\nu}} G(L^{\frac{1}{\nu}}(p - p_c)) + \text{corrections to scaling} \tag{1.7}$$

[31, 53], where β is the critical exponent for the approach to zero of the fraction of sites belonging to the infinite cluster in an infinite system as $p \searrow p_c$. Using the hyper-scaling relation $d = 2\frac{\beta}{\nu} + \frac{\gamma}{\nu}$ we see that (1.5), (1.6) and (1.7) lead to the scaling form (1.5)

being valid for all $|p-p_c| \ll 1$ and large L. That is on a finite system we do not need to differentiate between $p < p_c$ or $p > p_c$, we may include all the clusters when calculating $\Gamma_L(p)$.

Assuming (1.5) is valid for $|p-p_c| \ll 1$ the ratio $R_L = \frac{\Gamma_{2L}}{\Gamma_L}$ should become independent of L, for large L, at $p = p_c$. Plotting these ratios as a function of p for different sizes L and looking for the intersection of these different curves then yields p_c. The value of the ratios at the intersection point of the R_L curves should be equal to $2^{d+\frac{\gamma}{\nu}}$ giving us a way to measure $\frac{\gamma}{\nu}$. Moreover ,we also have

$$\frac{1}{\nu} = \frac{\ln\left(\frac{dR_{2L}}{dp} / \frac{dR_L}{dp}\right)}{\ln 2}. \tag{1.8}$$

Thus the slopes of these curves should also give ν.

In Fig. 3.1 we present results of the simulation for the massless harmonic crystal on a cubic lattice with periodic boundary conditions. Each Γ_L was averaged over 48000 samples except for $L = 160$ where the average is over 2400 samples. To determine the error bars we have divided the output of the simulations into 10 parts and assuming that the averages are Gaussian distributed we evaluated the variance which we used as a measure of the uncertainty. From the intersection of the curves, after interpolation, we obtain $p_c = 0.16 \pm 0.01$. Comparing the slopes of the R_L curves for $L = 80$ and $L = 40$ we obtain $\nu = 2.1 \pm 0.5$. From the value of R_L at the intersection point of the curves we obtain $\frac{\gamma}{\nu} = 1.8 \pm 0.1$. We actually computed Γ_L for the sequences $L = 10, 20, 40, 80, 160$ and $L = 15, 30, 60, 120$. All the simulation results are consistent with what is plotted in Fig. 3.1 where we have used only part of these simulations since the plot is otherwise cluttered. These values clearly show that our system is in a different universality class from independent percolation since for the latter $\nu = 0.876 \pm 0.001$ and $\frac{\gamma}{\nu} = 2.045 \pm 0.001$ [54].

The above method is good for finding the percolation threshold and the ratio of critical exponents $\frac{\gamma}{\nu}$ but clearly does not give good results for ν. To obtain more precise result for the percolation correlation length exponent we evaluated the probability that there is a "wrapping cluster", i.e. one that wraps around the torus, for different densities p of occupied sites and different linear sizes L.

For fixed L we denote by p_c^{eff} the value of the density of occupied sites for which one half of the realizations will have such a wrapping cluster. This should obey the following scaling relation $p_c^{eff} - p_c \sim L^{-\frac{1}{\nu}}$ [31]. For sizes between 30 and 100 we evaluated p_c^{eff} from doing simulation in a range between $p = 0.13$ and $p = 0.25$ in steps of 0.005. For each such system 24000 samples were generated. The slope of $\ln(p_c^{eff} - p_c)$ versus $\ln(L)$ should give us ν. A plot of the results is presented in Fig. 4.1. The slope of the fitted straight line is 0.50 ± 0.01 which gives $\nu = 2.00 \pm 0.04$. This is in good agreement with the theoretical prediction $\nu = 2$ of Weinrib and Halperin [3].

We have used the obtained values of p_c, $\frac{\gamma}{\nu}$ and ν to draw Fig. 4.2 where we see a good collapse of the data points to a smooth curve.

We also calculated the ratio of the critical exponents $\frac{\beta}{\nu}$. We did this by finding the fraction of sites that belong to the largest cluster in a system of linear size L, $\frac{P(p_c,L)}{L^d}$,when we simulate at the approximate critical density. From (1.7) we see that $\frac{P(p_c,L)}{L^d} \sim L^{-\frac{\beta}{\nu}}$. The result for systems of size from 40 to 170 averaged over 24000 samples is presented in (Fig. 4.3). From the slope of the fitted straight line we obtain $\frac{\beta}{\nu} = 0.60 \pm 0.01$. Moreover, the fact that $P(p_c, L)$ follows well a power law behavior supports our contention that the true critical value is near $p_c = 0.16 \pm 0.01$. Observe also that $2\frac{\beta}{\nu} + \frac{\gamma}{\nu} = 3.0 \pm 0.2$ and thus the hyper-scaling relation is satisfied.

4.2 The Voter Model

4.2.1 Formulation

Another system whose pair correlations decays like that of the massless harmonic crystal is the voter model in $\mathbb{Z}^d$ [11].

The voter model is defined through a stochastic time evolution. Each lattice site is occupied by a voter who can have two possible opinions, say yes or no. With rate τ^{-1} the voter at site x adopts the opinion of one of his/her $2d$ neighbors chosen at random. More specifically letting $\rho(x) = 0, 1$, $x \in \mathbb{Z}^d$, the time evolution of the voter model is specified by giving the rate $C_v(x, \rho)$ for a change at site x when the configuration is

given by ρ

$$C_v(x,\rho) = \frac{1}{\tau}\left[1 - \frac{1}{2d}(2\rho(x)-1)\sum_{|y-x|=1}(2\rho(y)-1)\right]$$

where τ sets the unit of time.

It is clear that for the voter model on a finite set $\Lambda \subset \mathbb{Z}^d$ with periodic or free boundary conditions (b.c.), there will be only two possible stationary states: either $\rho(x) = 1$ or $\rho(x) = 0$ for all $x \in \Lambda$. The same is true for the voter model on an infinite lattice in one and two dimensions: the only stationary states are the consensus states. However for $d \geq 3$ there are, as for the massless harmonic crystal, unique stationary states for every density p of positive spins, $p = \langle\rho(x)\rangle$. The correlations in this state decay as

$$\langle\rho(x)\rho(y)\rangle - p^2 = p(1-p)G_d(x-y)$$

where $G_d(x)$ is the probability for a random walker, starting at $x \in Z^d$, to hit the origin before escaping to infinity. It is well known that $G_d(x) \sim \frac{1}{|x|^{d-2}}$ for $d \geq 3$, i.e the pair correlation for the voter model has the same long range behavior as the massless harmonic crystal.

4.2.2 Simulation Method

An efficient method to simulate the voter model is to consider a box $B_{\mathcal{L}}$ of linear size $\mathcal{L}$ with stochastic boundary conditions, i.e. when a voter looks at the boundary he sees 1 with probability p and 0 with probability $1-p$. It is then possible to show that the distribution of the configuration of voters in a box B_L of size $L < \mathcal{L}$ centered inside $B_{\mathcal{L}}$ and far away from the boundary will approach the steady state measure (restricted to B_L) with density p for the voter model when $\mathcal{L} \to \infty$. In order to sample from the measure for the voter model inside $B_{\mathcal{L}}$ with such stochastic boundary conditions we use the following algorithm: Start a random walk from each site of B_L and let these random walks move independently until two of them meet in which case they coalesce. When a random walk hits the boundary of $B_{\mathcal{L}}$ it is frozen. We continue this until all the random walkers either coalesce or are frozen. After this is done we independently for each frozen

walker, assign the value 1 with probability p and the value 0 with probability $1-p$, then assign that same value to its ancestors, that is all the random walkers that have coalesced with it. In this way we assign values 1 or zero to all the sites in B_L. One can prove that in this way we sample configurations inside B_L with the distribution coming from the voter model in $B_{\mathcal{L}}$ with the stochastic boundary conditions discussed above see the Appendix. The advantage of this way of simulating is that one is guaranteed that the sampling is from the steady state measure with these boundary conditions.

4.2.3 Results

Using this method of generating configurations inside B_L for different p we looked for a spanning cluster inside B_L. We did simulations for sizes $L = 10, 15, 20, 25$ and 30 with $\mathcal{L} = 160$. The results which are the same for all $\mathcal{L}$ in the range $(120, 160)$ are presented in Fig. 4.4. If we assume the scaling form for the spanning probability [31]

$$\Pi_L(p) = F((p - p_c)L^{1/\nu}) \tag{2.1}$$

then by collapsing the data Fig. 4.5 we obtain $p_c = 0.10 \pm 0.01$ and $\nu = 2 \pm 0.2$.

To find $\frac{\gamma}{\nu}$ we measured $\frac{\Gamma_L}{L^3}$ and we assume the scaling form (1.5). Note that in this case we do not have periodic boundary conditions. Results from the simulation are presented in Fig. 4.6. Collapsing the data Fig. 4.7 we obtain $p_c = 0.10 \pm 0.01$, $\frac{\gamma}{\nu} = 1.9 \pm 0.2$ and $\nu = 2 \pm 0.2$.

Analogous simulation measurements for $P(p, L)$ gave $\frac{\beta}{\nu} = 0.6 \pm 0.1$. As in the case of the massless harmonic crystal the exponents we found satisfy the hyper-scaling relation $2\frac{\beta}{\nu} + \frac{\gamma}{\nu} = d$. The exponents for both the massless harmonic crystal and voter model seem to agree within the error bars.

4.2.4 Comparison of p_c with previous simulations

The percolation transition in the $d = 3$ voter model was first investigated in [48]. This was done by considering voters who occasionally change their opinions spontaneously, i.e. independently of what their neighbors are doing. They do this with probability λ.

In terms of flip rates one has

$$C(x,\rho) = (1-\lambda)C_v(x,\rho) + \frac{\lambda}{\tau}\left[1 + (1-2p)(2\rho(x)-1)\right],$$

where $0 \leq p \leq 1$ and $0 \leq \lambda \leq 1$ and C_v is the voter model flip rates. This leads to a stationary state in any periodic box of size L^d with density of pluses equal to p. As λ increases from 0 to 1 we go from the voter model to an independent flip model. The stationary state of the latter is a product measure with density p. This model was studied rigorously in [55] where it was named the noisy voter model.

In [48] the authors used (1.5) on simulation results of the noisy voter model on lattices with periodic boundary conditions to obtain $p_c(\lambda)$ for $\lambda > 0.1$. For $d = 3$ they found by extrapolation $p_c(\lambda) \sim 0.16$ as $\lambda \to 0$.

We have repeated the simulations in [48] for larger lattice sizes and smaller values of λ. We simulated systems with λ as small as 0.01 each with 24000 "effectively uncorrelated" samples and sizes up to 80. From our results we can extrapolate $p_c(\lambda) \to 0.15$ as $\lambda \to 0$, a value slightly lower than the result in [48]. We also observed that, as expected, the critical exponents for the noisy voter model agree, for the given range of λ, with the critical exponents of independent percolation.

This leaves a significant difference with the result for p_c obtained in the previous section. We believe that the answer lies in the necessary extrapolation to $\lambda = 0$. Since the autocorrelation time grows exponentially with lambda, this means we have to wait for more and more Monte Carlo steps to get independent samples. To check this explanation we investigated the percolation transition in the harmonic crystal with a mass M. This mass acts much like the random flips in the voter model. For both models the pair correlation decays exponentially. In the harmonic crystal the characteristic length scale is $\xi_M = \frac{1}{M}$. An easy calculation shows that the characteristic length scale for the noisy voter model is $\xi_\lambda = \sqrt{\frac{1-\lambda}{6\lambda}}$. The noisy voter model with the smallest lambda that we simulated , $\lambda = 0.01$, thus corresponds to ξ_λ roughly equal to 4 (unit distance is the lattice spacing). In the language of the massive harmonic crystal this corresponds to $M \sim 0.25$. Estimating the percolation threshold of the massless harmonic crystal by the extrapolation method we used for the voter model using $M \geq 0.25$ yields a

$p_c(M) \sim 0.21$ when $M \to 0$. This is obviously a large overestimate of $p_c = 0.16$ which was obtained by directly simulating the massless harmonic crystal. This shows that the extrapolation method greatly overestimates the true p_c.

4.3 Conclusion

We have performed Monte Carlo simulations to obtain the critical percolation density and some critical exponents for the massless harmonic crystal and the voter model in $\mathbb{Z}^3$. We found for the first time a value of p_c for the former and, using a novel method of simulation for the voter model, found a new more reliable value of p_c for this system. The critical exponents for both models agree within the error bars. This suggests that both percolation models are in the same universality class and confirms the theoretical predictions made in [3]. The result for the correlation length critical exponent $\nu = 2$ supports the conjecture by WH that the relation $\nu = \frac{2}{a}$ is exact.

It is believed that not only the critical exponents but also the finite size scaling functions are universal. While this is certainly consistent with our simulations we have not checked this carefully. Such a check would require measuring quantities for the two systems in the same way. This is not what we have done here as we wanted to use the most efficient method for each system.

We mention here that there has been much activity in generalizing the voter model in various ways [56]. Based on our present work we expect that the nature of the percolation transition in these models will depend only on the asymptotic behavior of $G(r)$. We have however not investigated this. Our simulation method may be extendable to some of these systems.

4.4 Appendix

4.4.1 The Voter Model with stochastic boundary conditions and its dual description

The notation and style of arguments are borrowed from [11]. Let $\Lambda = (0, L)^3$ and $\partial\Lambda$ be the boundary of Λ. Define $\partial\bar{\Lambda}$ to be the set which we obtain from $\partial\Lambda$ when each point $y \in \partial\Lambda$ is substituted with two points y_0 and y_1. Let's introduce the following function on configurations of the voter model

$$H(\eta, A) = \prod_{x \in A} [1 - \eta(x)] \tag{4.1}$$

with the product over the empty set defined to be equal to 1. Here, $\eta \in \{0, 1\}^{\Lambda}$ is a configuration of the voter modela and Λ is a subset of $\Lambda \cup \partial\bar{\Lambda}$. $E^{\eta}H(\eta_t, A)$ is the probability that at time t all of the voters with $x \in A$ have spin 0 given that at time 0 the configuration is η. From this probabilities we can construct the probabilities for any finite configuration of spins. For example we calculate the probability $P(E)$ of the event E that at time t , $\eta(x_1) = 0, \eta(x_2) = 1$ and $\eta(x_3) = 0$ for $x1, x2$ and $x3 \in \Lambda$ as follows. Introduce the sets $A = \{x1, x2, x3\}$ and $A^{'} = \{x1, x3\}$, we have the following:

$$P(E) = E^{\eta}H(\eta_t, A^{'}) - E^{\eta}H(\eta_t, A). \tag{4.2}$$

Here we are dealing with a voter model with stochastic boundary conditions (b.c.). These b.c. are defined as follows, whenever a voter looks at somebody beyond Λ he adopts an opinion 1 with prob p and opinion 0 with prob $1 - p$. To deal with this we have introduced the set $\partial\bar{\Lambda}$. If the voter looks at the boundary point y he sees the voter at y_0 with probability 1-p and the voter at y_1 with probability p, $\eta(y_1)$ and $\eta(y_0)$ are fixed to be always 1 and 0 respectively. The flip rates for the voter model with stochastic b.c. are defined as

$$c(x, \eta) = \sum_{y \in N_x \cap \Lambda} \frac{1}{2d}\eta(y) + |N_x \cap \partial\Lambda|\frac{1}{2d}p \quad \text{if} \quad \eta(x) = 0, \tag{4.3}$$

$$c(x, \eta) = \sum_{y \in N_x \cap \Lambda} \frac{1}{2d}(1 - \eta(y)) + |N_x \cap \partial\Lambda|\frac{1}{2d}(1 - p) \quad \text{if} \quad \eta(x) = 1. \tag{4.4}$$

$$\tag{4.5}$$

The voters at the boundary are stationary, that is $c(y,\eta) = 0$ for $y \in \partial\bar{\Lambda}$. We can rewrite the rates for the voter model with a stochastic boundary as follows

$$c(x,\eta) = (1-\eta(x)) + (2\eta(x)-1)\sum_{y\in N_x} p(x,y)H(\eta,y) \tag{4.6}$$

where $p(x,y)$ is the transition rate for a random walk that is absorbed on the boundary. For $x \in \Lambda$ and $N_x \cap \partial\Lambda$ empty, N_x is the set of nearest neighbors for site x, $p(x,y)$ is the transition rate for a simple n.n. random walk that is for every $y \in N_x$, $p(x,y) = \frac{1}{2d}$ and for $y \notin N_x$ $p(x,y) = 0$. For $x \in \Lambda$ and $N_x \cap \partial\Lambda$ not empty $p(x,y) = \frac{1}{2d}$ for all $y \in \Lambda \cap N_x$, then in addition for every $y \in N_x \cap \partial\Lambda$ we have $p(x,y_1) = \frac{p}{2d}$ and $p(x,y_0) = \frac{1-p}{2d}$. For $x \in \partial\bar{\Lambda}$, $p(x,y) = 1$ if $x = y$ and $p(x,y) = 0$ otherwise. Notice that for all $x \in \Lambda \cup \partial\bar{\Lambda}$ this definition gives $\sum_{y\in N_x} p(x,y) = 1$.

Observe that.

$$H(\eta_x, A) - H(\eta, A) = (2\eta(x)-1)H(\eta, A\setminus x) \quad if \quad x \in A$$
$$H(\eta_x, A) - H(\eta, A) = 0 \quad if \quad x \notin A$$

η_x is the configuration that is obtained from "flipping" the spin at position x.

$$H(\eta,A)H(\eta,B) = H(\eta, A\cup B)$$

Next we apply the generator to the function H and see how it evolves.

$$\begin{aligned}
\Omega H(\eta,A) = \sum_{x\in\Lambda} c(x,\eta)[H(\eta_x,A) - H(\eta,A)] = \\
\sum_{x\in\Lambda}[1-\eta(x) + (2\eta(x)-1)\sum_{y\in N_x} p(x,y)H(\eta,y)][H(\eta_x,A) - H(\eta,A)] = \\
\sum_{x\in\Lambda\cap A}[1-\eta(x) + (2\eta(x)-1)\sum_{y\in N_x} p(x,y)H(\eta,y)](2\eta(x)-1)H(\eta, A\setminus x)] = \\
\sum_{x\in\Lambda\cap A}[(1-\eta(x))(2\eta(x)-1)H(\eta,A\setminus x) + \sum_{y\in N_x} p(x,y)H(\eta,y)H(\eta,A\setminus x)] = \\
\sum_{x\in\Lambda\cap A}[-H(\eta,A) + \sum_{y\in N_x} H(\eta,(A\setminus x)\cup y)] = \\
\sum_{x\in\Lambda\cap A}\sum_{y\in N_x} p(x,y)[H(\eta,(A\setminus x)\cup y) - H(\eta,A)] = \\
\sum_{B} q(A,B)[H(\eta,B) - H(\eta,A)]
\end{aligned}$$

Here $q(A,B) = \sum_{x\in\Lambda\cap A}\sum_y p(x,y)$ where the sum over y is over all $y \in N_x$ such that $(A \setminus x) \cup y = B$. Now $q(A,B)$ can be interpreted as a transition rate for a continuous time Markov chain on Y(set of all subsets of $\Lambda \cup \partial\bar{\Lambda}$) which evolves in the following way.

1. Each $x \in \Lambda \cap A$ is removed from A with a rate 1 and is replaced with y with a probability $p(x,y)$.

2. When an attempt is made to put a point at a site which is already occupied, then the points coalesce. Clearly this process will end once all the points are replaced with points from the boundary. Now we can use a theorem from [11] and conclude that

$$\hat{\mu}_t(A) = \sum_{B\in Y} E^A[A_t = B]\hat{\mu}(B) \tag{4.7}$$

Here $\hat{\mu}(A) = \int H(\eta, A)\mu(d\eta)$ and $\mu_t = \mu S(t)$ (μ is a measure on spin configurations in $\Lambda \cup \partial\bar{\Lambda}$). If we take $t \to \infty$ in the above equation we obtain

$$\hat{\mu}_\infty(A) = \sum_{B\in Y} E^A[A_\tau = B]\hat{\mu}(B). \tag{4.8}$$

Here τ is the stopping time measuring the time when the last random walk hits the boundary. We conclude that in (4.8) the only contribution comes from $B \in Y_{\partial\bar{\Lambda}}$ where $Y_{\partial\bar{\Lambda}}$ is the set of all subsets of $\partial\bar{\Lambda}$. Note that τ is necessarily finite.

Since once a walker hits a boundary point y he chooses to move to point y_0 or y_1 each time independently with probability $1-p$ and p respectively then we can modify (4.8) as follows

$$\hat{\mu}_\infty(A) = \sum_{B\in Y_{\partial\Lambda}} E^A[\mathrm{mod}(A_\tau) = B](1-p)^{|B|}. \tag{4.9}$$

where now $Y_{\partial\Lambda}$ is the set of all subsets of $\partial\Lambda$ and $\mathrm{mod}(A_\tau)$ is the set obtained from A_τ by substituting every y_0 or y_1 with y, and thus $\mathrm{mod}(A_\tau) \in Y_{\partial\Lambda}$. Using this formula we can show that the probability that $x_1 = 0, x_2 = 0, x_3 = 1$ (event E) say is given by the following formula

$$\begin{aligned} P(E) = P(\text{random walks starting at } \ x_1, x_2 \text{ coalesce but not } x3)(1-p)p \\ +P(\text{none of the walkers coalesce})(1-p)^2p \end{aligned}$$

Using induction we can prove a formula like that for a general situation.

4.4.2 Correlations for the level field of a Gaussian field

Let ϕ be a general translation and rotation invariant Gaussian Field on $\mathbb{Z}^d$ with $\langle\phi\rangle = 0$ and $g(r) = \langle\phi(x)\phi(y)\rangle$ where $r = |x-y|$. Let us define a percolation field η as follows

$$\eta(x) = \begin{cases} 1 & \phi(x) \geq h \\ 0 & \phi(x) < h \end{cases}$$

That is $\eta(x) = H(\phi(x) - h)$ where H is the Heaviside step function. Then we have

$$\langle\eta(x)\rangle = \frac{1}{\sqrt{2\pi g(0)}} \int_h^\infty e^{-\frac{u^2}{2g(0)}} du \tag{4.10}$$

One can also calculate any order of the correlation functions, here we are interested in the two point correlations $\langle\eta(x)\eta(y)\rangle$. To do the calculation we use an integral representation of the Heaviside step function

$$H(x) = \lim_{\epsilon\to 0^+} -\frac{1}{2\pi i}\int_{-\infty}^{\infty} \frac{1}{\tau + i\epsilon} e^{-ix\tau} d\tau. \tag{4.11}$$

Using this representation one obtains

$$\begin{gathered} \langle\eta(x)\eta(y)\rangle = \langle H(\phi(x)-h)H(\phi(y)-h)\rangle = \\ \langle \frac{1}{(2\pi i)^2}\int_{C_1} e^{-i\tau_1(\phi(x)-h)}\frac{d\tau_1}{\tau_1}\int_{C_2} e^{-i\tau_2(\phi(y)-h)}\frac{d\tau_2}{\tau_2}\rangle = \\ \int_{-\infty}^{\infty} d\phi(x)\int_{-\infty}^{\infty} d\phi(y)\frac{1}{2\pi|\Sigma|^{1/2}} e^{-\frac{1}{2}\phi^T\Sigma^{-1}\phi} \\ \frac{1}{(2\pi i)^2}\int_{C_1} e^{-i\tau_1(\phi(x)-h)}\frac{d\tau_1}{\tau_1}\int_{C_2} e^{-i\tau_2(\phi(y)-h)}\frac{d\tau_2}{\tau_2} \end{gathered}$$

In the above equation C_1 and C_2 are contours along the real axis which avoid the origin by crossing the imaginary axis in the upper half plane, ϕ is a 2d vector with components $\phi(x)$ and $\phi(y)$ and Σ is the correlation matrix $\begin{pmatrix} g(0) & g(|x-y|) \\ g(|x-y|) & g(0) \end{pmatrix}$.

Interchanging the order of integration and performing the integration over ϕ and differentiating with respect to $g \equiv g(|x-y|)$ to simplify the remaining integrals one obtains

$$\frac{\partial\langle\eta(x)\eta(y)\rangle}{\partial g} = -\frac{1}{(2\pi i)^2}\int_{\infty}^{\infty} d\tau_1 \int_{-\infty}^{\infty} d\tau_2 e^{-\frac{1}{2}\tau^T\Sigma\tau + ih^T\tau}$$

where τ is the 2d vector with coordinates τ_1 and τ_2 and h is the 2d vector with coordinates h. After performing the integrations we obtain

$$\langle \eta(x)\eta(y)\rangle = p^2 + \frac{1}{2\pi}\int_0^{\frac{g(r)}{g(0)}} \frac{du}{\sqrt{1-u^2}} e^{-\frac{h^2}{1+u}} du$$

We have the p^2 term since if $g(r) = 0$ then necessarily $\langle \eta(x)\eta(y)\rangle = \langle \eta(x)\rangle\langle \eta(y)\rangle$. If $r \to \infty$ then $\frac{g(r)}{g(0)} \to 0$ so $\langle \eta(0)\eta(r)\rangle \to \frac{1}{2\pi} e^{-h^2}\frac{g(r)}{g(0)}$.

Now let us perform a similar calculation for another percolation field that we define as follows

$$\eta(x) = \begin{cases} 1 & |\phi(x)| > h \\ \\ 0 & |\phi(x)| < 0 \end{cases}$$

Notice that in this case the field can be represented in terms of Heviside functions as well

$$\eta(x) = 1 - H(\phi(x) - h) + H(\phi(x) + h).$$

One can proceed as in the previous case, performing very similar calculations one obtains

$$\langle \eta(0)\eta(r)\rangle = p^2 + \frac{1}{2\pi}\int_0^{\frac{g(r)}{g(0)}} \frac{1}{\sqrt{1-u^2}} (e^{-\frac{h^2}{(1+u)}} - e^{-\frac{h^2}{(1-u)}}) du$$

for $r \to \infty$ this simplifies to $\langle \eta(0)\eta(r)\rangle \sim p^2 + \frac{1}{2\pi}\frac{4g(r)^2h^2}{g(0)}$.

We are interested in the case when the Gaussian field is the Harmonic crystal in 3d. In this case $g(r) \sim \frac{1}{r}$ so for the first percolation field the correlations fall also as $\frac{1}{r}$ while for the second percolation field the correlations fall of as $\frac{1}{r^2}$.

4.4.3 Correlations for the Noisy Voter Model

Here we work with the spin variable $\sigma(x) = 2\rho(x) - 1$. The master equation for the model is given by

$$\frac{dP(\sigma,t)}{dt} = \sum_x [c(x,\sigma^x)P(\sigma^x,t) - c(x,\sigma)P(\sigma,t)] \tag{4.12}$$

Here σ^x is the configuration that is obtained from σ by a single spin flip at site x. One can derive a differential equations for the spin two point correlation functions

$\langle\sigma(x)\sigma(y)\rangle = \sum_\sigma \sigma(x)\sigma(y)P(\sigma,t)$.

$$\frac{d\langle\sigma(x)\sigma(y)\rangle}{dt} = (1-\lambda)[-4\langle\sigma(x)\sigma(y)\rangle + \frac{2}{z_d}\sum_{e_i}\langle\sigma(x)\sigma(y+e_i)\rangle + \frac{2}{z_d}\sum_{e_i}\langle\sigma(x+e_i)\sigma(y)\rangle] - \lambda[4\langle\sigma(x)\sigma(y)\rangle - 4\lambda(1-2p)^2]$$

In the steady state the left hand side of this equation should vanish. For large separation $|x-y|$ and assuming spherical symmetry the above equation can be rewritten as.

$$(1-\lambda)\Delta F(r) - 2ad\lambda + 2da\lambda(1-2p)^2 = 0 \tag{4.13}$$

where a is the lattice spacing.

In 3 dimensions and assuming spherical symmetry the Laplacian operator is very simple. Substituting solution of the form $F(r) = \frac{e^{-\frac{r}{k}}}{r} + C$. we get $k = \sqrt{\frac{1-\lambda}{6\lambda}}$ and $C = (1-2p)^2$. Since $<\sigma(0)>= 2p-1$ we get that the truncated two point correlation function for large separation r becomes $\frac{e^{-\frac{r}{k}}}{r}$.

This looks exactly like the two point correlation function in the massive harmonic crystal model , if we identify k with $\frac{1}{M}$(M is the mass in the model).

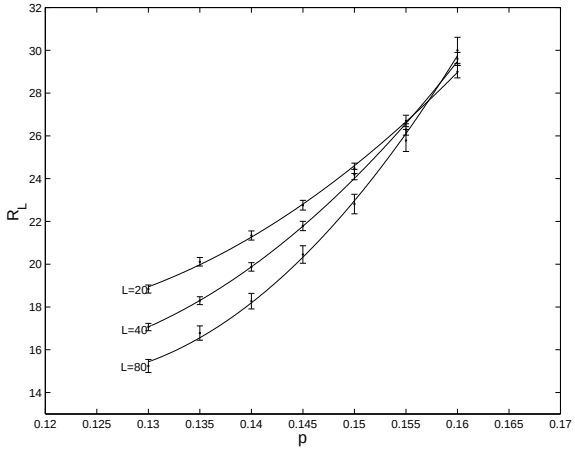

Figure 4.1: Plot of R_L versus p for the $d = 3$ massless harmonic crystal. We estimate $p_c = 0.16 \pm 0.01$

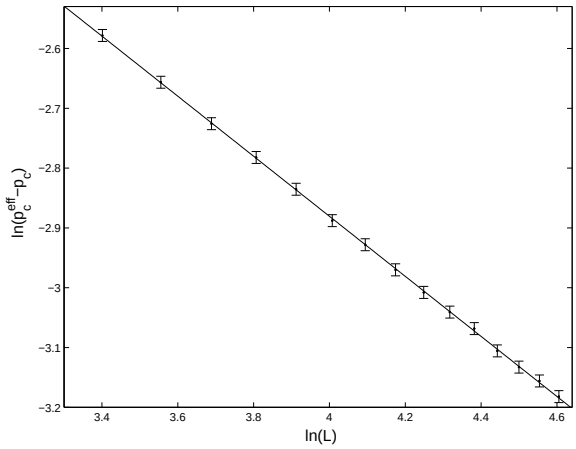

Figure 4.2: Plot of $\ln(p_c^{eff} - p_c)$ versus $\ln(L)$. The slope if the straight line gives $\nu = 2.00 \pm 0.04$

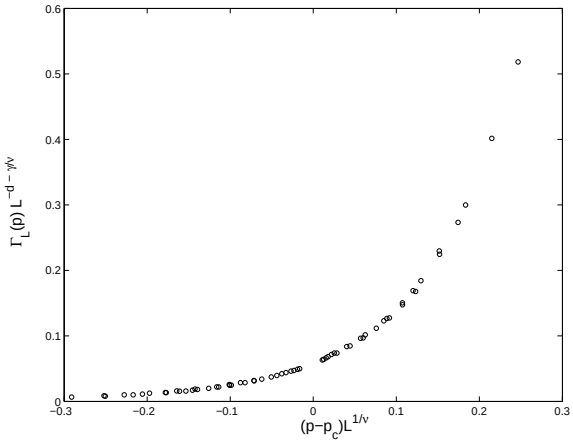

Figure 4.3: Plot of $\Gamma_L L^{-d-\frac{\gamma}{\nu}}$ versus $(p-p_c)L^{\frac{1}{\nu}}$ for the $d=3$ massless harmonic crystal for $p_c = 0.16$, $\nu = 2$ and $\frac{\gamma}{\nu} = 1.8$. We have plotted data points for $L = 30, 60, 120$ for $p = 0.13$ to 0.16 in steps of 0.005 and for $L = 40, 80, 160$ for $p = 0.13$ to 0.18 in steps of 0.005.

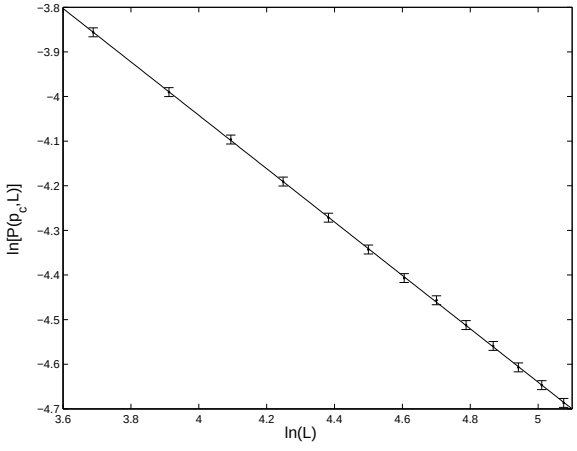

Figure 4.4: Plot of $\ln[P(p_c, L)]$ versus $\ln(L)$. The slope of the straight line gives $\frac{\beta}{\nu} = 0.60 \pm 0.01$

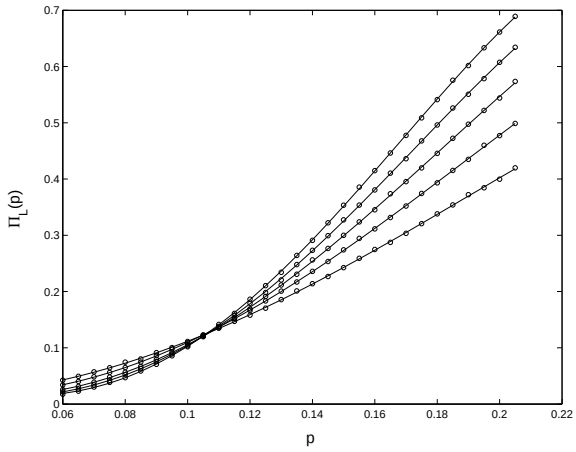

Figure 4.5: Plot of Π_L versus p for the $d = 3$ voter model. We have plotted data points for $L = 10, 15, 20, 25$ and 30 from $p = 0.06$ to $p = 0.205$ in steps of 0.005. Each point is an average over 10^5 samples. The error bars are not shown since on this scale they are too small.

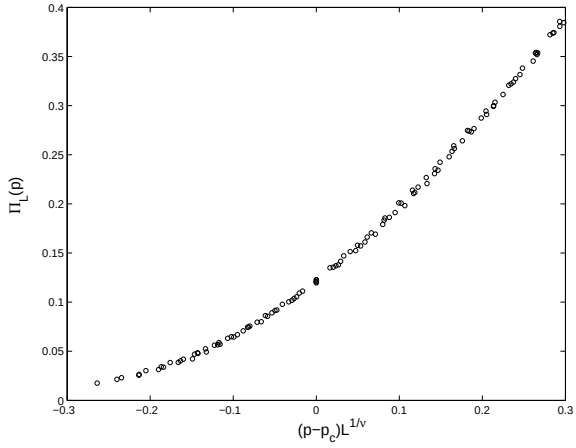

Figure 4.6: Plot of Π_L versus $(p - p_c)L^{\frac{1}{\nu}}$ for the $d = 3$ voter model for $p_c = 0.105$ and $\nu = 2$. We have used the same data that was used to create Fig. 4.4

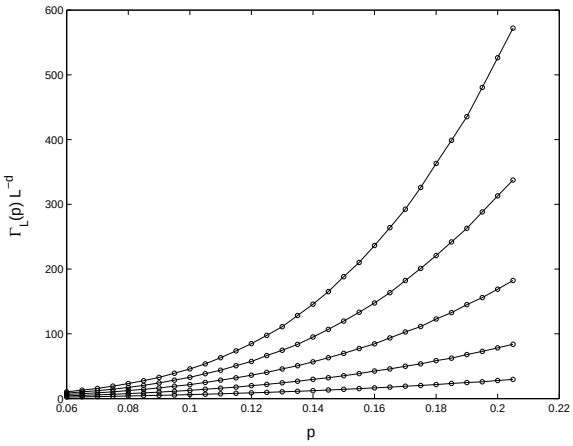

Figure 4.7: Plot of $\Gamma_L L^{-d}$ versus p for the $d = 3$ voter model. We have plotted data points for $L = 10, 15, 20, 25$ and 30 from $p = 0.06$ to $p = 0.205$ in steps of 0.005. Each point is an average over 10^5 samples. The error bars are not shown since on this scale they are too small.

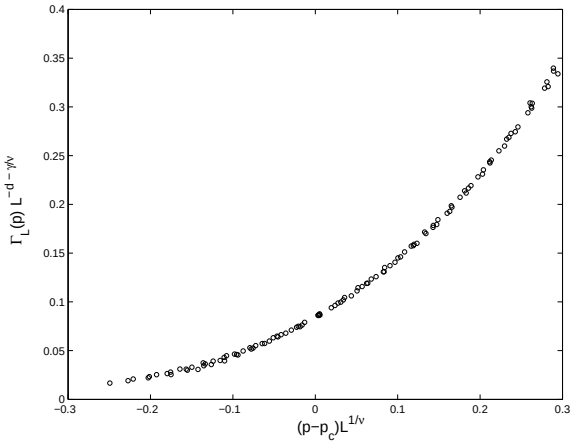

Figure 4.8: Plot of $\Gamma_L L^{-d-\frac{\gamma}{\nu}}$ versus $(p-p_c)L^{\frac{1}{\nu}}$ for the $d = 3$ voter model for $p_c = 0.105$, $\nu = 2$ and $\frac{\gamma}{\nu} = 1.9$. We have used the same data that was used to create Fig. 4.6

Chapter 5

Conclusion

Percolation is a vast and interesting subject. In this thesis we discussed dependent percolation models. We used the disordered Potts ferromagnet to provide examples of models for which the critical percolation density can be pushed arbitrarily close to 0 or 1. We then introduced the long range correlated percolation models. Using momentum space RG we attempted computing the critical exponents associated with the percolation transition, the results did not compare well with our Monte Carlo simulation. However, the RG calculation confirmed that introducing long range correlations changes the critical exponents in the percolation transition. This was also confirmed in the context of two specific models, the Harmonic Crystal and Voter model in $3d$. For a broad overview of percolation and various interesting research direction see [31].

We would like to outline two further research directions that might be of interest. In $2d$ the critical q-state Potts models can be identified with the minimal conformal models that are parametrised by an integer m which determines the central charge and critical behavior of the model [57]. The correspondence is given by

$$m = \frac{\pi}{\cos^{-1}\left(\frac{\sqrt{q}}{2}\right)} - 1 \tag{0.1}$$

The central charge and exponents are

$$\begin{aligned} c &= 1 - \frac{6}{m(m+1)} \\ x_\epsilon &= \frac{m+3}{2m} \\ x_\sigma &= \frac{(m+3)(m-1)}{8m(m+1)} \end{aligned} \tag{0.2}$$

here x_ϵ and x_σ are the thermal and magnetic scaling dimensions. Bond disorder can be introduced as a perturbation of this conformal field theory by an operator proportional

to the energy operator. After using the Replica trick to average over the disorder one obtains an effective Hamiltonian. This Hamiltonian can be further studied to determine whether this disorder results into a new critical behavior and if so calculate the new operator scaling dimensions. This has been done for short range correlations in [58]. We are interested in the study of long range correlations. In this case after averaging over the disorder using n replicas one obtains the following effective Hamiltonian

$$H_{eff} = H + g_0 \sum_{\alpha \neq \beta} \int \frac{\epsilon^{\alpha}(z_1)\epsilon^{\beta}(z_2)}{|z_1 - z_2|^a} dz_1 dz_2 \tag{0.3}$$

where α and β are any of the n replicas and ϵ^{α}, ϵ^{β} are the respective energy operators. One can then perform a perturbative expansion where the last term in (0.3) is considered a perturbation, renormalize etc. Notice however that if $q = 1$ then this perturbation is relevant if $a < \frac{3}{2}$. For $2d$ independent percolation it is rigorously known that the correlation length critical exponent is $\nu = \frac{4}{3}$ [30] we thus recover the generalized Harris criteria for long range correlated disorder. The disorder is relevant exactly when $a\nu - 2 < 0$.

Another interesting direction for exploration is to study SLE [59] in the context of appropriate disordered Potts ferromagnets for $q > 4$. For a study of SLE in the context of $q = 3$ Potts models see [60].

References

[1] A. Weinrib. Long range correlated percolation. *Phys Rev. B*, 29:387, 1984.

[2] M. Sahimi. *Applications of Percolation Theory.* Taylor Francis Ltd., London, 1994.

[3] A. Weinrib and B. Halperin. Critical phenomena in systems with long-range-correlated qenched disorder. *Phys. Rev. B*, 27:413, 1983.

[4] G. Grimmet. *Percolation.* Berlin, New York : Springer Verlag, 1999.

[5] J. Bricmont, J. Lebowitz, and C. Maes. Percolation in strongly correlated systems: The massless gaussian field. *Jour. Stat. Phys.*, 48:1249, 1987.

[6] G. Giacomin. private communication.

[7] R.M. Burton and M.S. Keane. Density and uniqueness in percolation. *Comm. Math. Phys.*, 121:501, 1989.

[8] C. M. Newman and L.S. Schulman. Infinite clusters in percolation models. *J. Stat. Phys.*, 26:613, 1981.

[9] H. O. Georgii, 0. Hägström, and C. Maes. The random geometry of equilibrium phases. In C. Domb and J.L. Lebowitz, editors, *Phase Transition and Critical Phenomena*, volume 18, page 1. Academic Press, London, 2001.

[10] L. Chayes, J. Lebowitz, and V. Marinov. Percolation phenomena in low and high density systems. arXiv: cond-mat/0701468, submitted for publication.

[11] T. M. Liggett. *Interacting Particle Systems.* New York : Springer Verlag, 1985.

[12] L. Chayes. Percolation and ferromagnetism on $\mathbb{Z}^2$: the q-state potts cases. *Stochastic Processes and Their Applications*, 65:209, 1996.

[13] O. Häggström. Positive correlations in the fuzzy potts model. *Annals of Applied Probability*, 9:1149, 1999.

[14] S. Adams and R. Lyons. Amenability, kazhdan's property and percolation for trees groups and equivalence relations. *Israel J. Math.*, 75:341, 1991.

[15] O. Häggström. Infinite clusters in dependent automorphism invariant percolation on trees. *Ann. Probab.*, 25:1423, 1997.

[16] I. Benjamini, R. Lyons, Y. Peres, and O. Schramm. Group invariant percolation on graphs. *Geom. Funct. Anal.*, 9:29, 1999.

[17] M. Aizenman, J.T. Chayes, L. Chayes, J. Fröhlich, and L. Russo. On a sharp transition from area law to perimeter law in a system of random surfaces. *Commun. Math. Phys.*, 92:19, 1983.

[18] A. C. D. van Enter, C. Maes, R. H. Schonmann, and S. B. Shlosman. The griffiths singularity random field. In R.A. Milnos, S. B. Shlosman, and Yu. M. Suhov, editors, *On Dobrushin's way: from probability theory to statistical physics*, page 51. Providence, RI, USA, 2000.

[19] C. M. Fortuin and P. W. Kasteleyn. On the random-cluster model. i. introduction and relation to other models. *Physica*, 57:536, 1972.

[20] Robert B. Griffiths and A. C. D. van Enter. The order parameter in a spin glass. *Comm. Math. Phys.*, 90(3):319, 1983.

[21] M. Aizenman, J. T. Chayes, L. Chayes, and C. M. Newman. Discontinuity of the magnetization in one-dimensional $1/|x-y|^2$ ising and potts models. *J.Stat.Phys.*, 77:351, 1988.

[22] M. Aizenman, J. T. Chayes, L. Chayes, and C. M. Newman. The phase boundary in dilute and random ising and potts ferromagnets. *J. Phys. A: Math. Gen.*, 20:20, 1987.

[23] L. Chayes and K. Shtengel. Critical behavior of $2d$ uniform and disordered ferromagnets at self-dual points. *Comm. Math. Phys.*, 204:353, 1999.

[24] T. Baker and L. Chayes. On the unicity of discontinuous transitions in the two-dimensional potts and ashkin–teller models. *Jour. Stat. Phys.*, 93:1, 1998.

[25] M. Aizenman and J. Wehr. Rounding effects of quenched randomness on first–order phase transitions. *Comm. Math. Phys.*, 130:489, 1990.

[26] J. M. Schwarz, A. J. Liu, and L. Q. Chayes. The onset of jamming as the sudden emergence of an infinite k-core cluster. *Europhys. Lett.*, 73:560, 2006.

[27] D. J. Thouless. Long range order in one-dimensional ising systems. *Phys. Rev.*, 187:732, 1969.

[28] S. Chakravarty. Quantum fluctuations in the tunneling between superconductors. *Phys. Rev. Lett.*, 49:681, 1982.

[29] J. Z. Imbrie and C. M. Newman. An intermediate phase with slow decay of correlations in one dimensional $1/|x-y|^2$ percolation, ising and potts models. *Commun. Math. Phys.*, 118:303, 1988.

[30] S. Smirnov. Critical percolation in the plane: Conformal invariance, cardy's formula, scaling limits. *C. R. Acad. Sci. Paris*, 333:239, 2001.

[31] D. Stauffer and A. Aharony. *Introduction to Percolation Theory*. Taylor Francis, New York, 1994.

[32] H. K. Janssen and Uwe C. Tauber. The field theory approach to percolation processes. *Ann. Phys.*, 315:147, 2005.

[33] R.G. Priest and T.C.Lubensky. Critical properties of two tensor models with application to the percolation problem. *Phys. Rev. B*, 13:4159, 1976.

[34] F. Fucito and E. Marinari. Computation of the critical exponents of percolation. *J. Phys. A: Math. Gen.*, 14:L85, 1981.

[35] J. Cardy and P. Grassberger. Epidemic models and percolation. *J. Phys. A: Math. Gen.*, 18:L267, 1985.

[36] H. K. Janssen. Renormalized field theory of dynamical percolation. *Z. Phys. B*, 58:311, 1985.

[37] H. K. Janssen. Renormalized field theory of the gribov process with quenched disorder. *Phys. Rev. E*, 55:6253, 1997.

[38] G. Parisi. Field-theoretic approach to second-order phase transitions in two- and three-dimensional systems. *J. Stat. Phys.*, 23:49, 1980.

[39] V.V. Prudnikov, P.V. Prudnikov, and A.A. Fedorenko. Field-theory approach to critical behavior of systems with long-range correlated defects. *Phys. Rev. B*, 62:8777, 2000.

[40] J. Benzoni and J.L.Cardy. A hyperscaling relation in site-bond correlated percolation. *J. Phys. A: Math. Gen.*, 17:179, 1984.

[41] D.J. Amit. *Field Theory, The Renormalization Group and Critical Phenomena*. World Scientific, Singapore, 1984.

[42] V. Marinov and J. Lebowitz. Percolation in the harmonic crystal and voter model in three dimensions. *Phys. Rev. E*, 74:031120, 2006.

[43] G. Paul, R.M. Ziff, and H.E. Stanley. Percolation threshold, fisher exponent, and shortest path exponent for four and five dimensions. *Phys Rev. E*, 64:026115, 2001.

[44] N. Breuer and H. K. Janssen. Equation of state and dynamical properties near the yang-lee edge singularity. *Z. Phys. B*, 41:55, 1981.

[45] G.A. Baker, B.G. Nickel, and M.S. Green amd D.I.Meiron. Ising-model critical indices in 3 dimensions from the callan-symanzik equation. *Phys. Rev. Lett.*, 36:1351, 1976.

[46] J.B.Bronzan and J.W.Dash. Higher-order ϵ terms in reggeon field theory. *Phys. Rev. D*, 10:4208, 1974.

[47] S. Prakash, S. Havlin, M. Schwartz, and H.E. Stanley. Structural and dynamical properties of long-range correlated percolation. *Phys. Rev. A*, 46:R1724, 1992.

[48] J. Lebowitz and H. Saleur. Percolation in strongly correlated systems. *Physica A: Math. Gen.*, 138:194, 1985.

[49] H.-O. Georgii. *Gibbs Measures and Phase Transitions*. de Gruyter Studies in Mathematics 9 (Walter de Gruyter & Co., Berlin), 1988.

[50] R. Fernandez A. van Enter and A. Sokal. Regularity properties and pathologies of position-space renormalization-group transformations: Scope and limitations of gibsian theory. *Jour. Stat. Phys.*, 72:879, 1993.

[51] S. Sheffield. Gaussian free fields for matematicions. arXiv: math.PR/0312099.

[52] H. Saleur and B. Derrida. A combination of monte carlo and tranfer matrix methods to study 2d and 3d percolation. *J. Physique*, 46:1043, 1985.

[53] K. Binder and D.W. Heermann. *Monte Carlo Simulation in Statistical Physics: An Introduction*. Springer-Verlag,Berlin, 1992.

[54] H. G. Ballesteros, L. A. Fernandez, V. Martin-Mayor, A. Munoz Sudupe, G. Parisi, and J.J. Ruiz-Lorenzo. Scaling corrections: Site-percolation and ising model in three dimensions. *J. Phys A: Math. Gen.*, 32:1, 1999.

[55] B. Granovsky and N. Madras. The noisy voter model. *Stochastic Processes and Their Application*, 55:23, 1995.

[56] I. Dornic, H. Chate, J. Chave, and H. Hinrichsen. Critical coarsening without surface tension: The universality class of the voter model. *Phys. Rev. Lett.*, 87:045701, 2001.

[57] B. Bertrand and C. Christophe. Phase transitions in two-dimensional random potts models. In Yu. Holovatch, editor, *Order,disorder and criticality*, page 146. World Scientific, Singapore, 2004.

[58] V. Dotsenko, M. Picco, and P. Pujol. Renormalization group calculation of correlation functions for the 2d random bond ising and potts models. *Nucl. Phys. B*, 455:701, 1995.

[59] J. Cardy. Sle for theoretical physicist. *Annals Phys.*, 318:81, 2005.

[60] A. Gamsa and J. Cardy. Sle in three-state potts model-a numerical study. arXiv: 0705.1510.

Vita

Vesselin Marinov

2001-2007 Ph. D. in Physics, Rutgers University

2006-2007 M.Sc. in Mathematics, option in Mathematical Finance, Rutgers University

1997-2001 B.Sc. in Mathematics, Massachusetts Institute of Technology (MIT)

1996-97 Physics Department, Sofia University, Sofia , Bulgaria. Transfered to MIT

1996 Graduated from Model Secondary School of Mathematics "Academic Kiril Popov", Plovdiv , Bulgaria.

2006-2007 Teaching assistant, Department of Physics, Rutgers University

2004-2006 Graduate assistant, Department of Physics, Rutgers University

2001-2004 Teaching assistant, Department of Physics, Rutgers University

Publications

1. V. Marinov and J. Lebowitz. Percolation in the harmonic crystal and voter model in three dimensions. *Phys. Rev. E*, 74:031120, 2006.

2. L. Chayes, J. Lebowitz, and V. Marinov. Percolation phenomena in low and high density systems. arXiv: cond-mat/0701468, submitted for publication.

3. V. Marinov. Long range correlated percolation. arXiv: cond-mat/0611533, submitted for publication.

4. O. Artoun, et. al. Seismic imaging, one-way wave equations, pseudodifferential operators, path integrals and all that jazz. *AIP Conference Proceedings*, 834:286, 2006.

5. H. Gao, T. -S. H. Lee and V. Marinov. $\phi - N$ bound state *Phys. Rev. C*, 63:022201, 2001.